I give permission for public access to my thesis and for copying to be done at the discretion of the archives' librarian and/or the College library.

_____ _____

Signature Date

Mmp2 as a Regulatory Target of *ßftz-f1* in *Drosophila melanogaster* Larval Fat Body Remodeling

By

Lillian Katz

A Paper Presented to the

Faculty of

Mount Holyoke College in

Partial Fulfillment of the Requirements for

the Degree of Bachelors of Arts with

Honor

Department of Biological Sciences

South Hadley, MA 01075

April 2015

This paper was prepared
under the direction of
Professor Craig Woodard
for eight credits.

DEDICATION

To Mount Holyoke College:

This institution has provided me with more opportunities than I ever believed possible. Thank you for helping me to achieve dreams that I didn't even know I had.

To future women in science:

Seize your opportunities and speak up for yourself. If you choose to be, you are capable of achieving seemingly unreachable goals.

ACKNOWLEDGEMENTS

First and foremost, I would like to thank Mount Holyoke College for providing me with the opportunity and the resources to carry out this project. Specifically, I would like to thank the Mount Holyoke Biological Sciences department for their resources, support, and inspiration.

Secondly, I would like to thank my project advisor Professor Craig Woodard. Thank you for giving me this incredible opportunity. You have supported me and pushed me further than I have ever been pushed while always believing in my ability to succeed. I have learned so much working in the Woodard lab.

Thank you to the other members of the thesis committee Amy Camp, and Maria Gomez. I truly appreciate the time and support you have put forth towards furthering my education.

Thank you to my fellow members of the Woodard lab. It's always uplifting to see a smiling face at midnight while surrounded by *Drosophila* prepupae. And thank you to Liz Mearls for your assistance with MxPro and qPCR data analysis.

Thank you to my friends and family for your continued love, support, proofreading, and encouraging words. And thank you to Gabby for your endless reassurance, kindness, love, and countless late nights spent in the biology department lounge waiting up for PCR reactions.

TABLE OF CONTENTS

LIST OF FIGURES

LIST OF TABLES

ABSTRACT

Tissue remodeling is an important process by which cells dissociate and detach from one another. This phenomenon is involved in both healthy and disease driven functions in the human body including wound healing, and cancer metastasis. Tissue remodeling is carried out in part by Matrix Metalloproteinases (MMPs), proteases that cleave bonds in extracellular matrix (ECM) allowing cells to dissociate and detach from one another, enabling them to move to new locations. Due to the potentially dangerous actions of *Mmps*, their expression is tightly regulated. *Drosophila melanogaster* is a useful model organism for studying tissue remodeling and the regulation of *Mmp* expression through the examination of larval fat body remodeling.

Drosophila larval fat body remodeling occurs during the transition from larva to adult fly. It is a tightly regulated process believed to involve the MMP Matrix Metalloproteinase 2 (MMP2). MMP2 is thought to cleave fat cell ECM proteins allowing cells to detach from each other in the process of remodeling. Previous research suggests that *Mmp2* expression in *Drosophila* is regulated by a ßFTZ-F1-mediated, 20-hydroxyecdysone (ecdysone) hormonal cascade (Bond et al. 2011). Both *ßftz-f1* and *Mmp2* have been demonstrated as necessary and sufficient to induce *Drosophila* larval fat body remodeling (Bond et al. 2011). This study investigates the hypothesis of *Mmp2* as a downstream regulatory target of ßFTZ-F1 as a part of an ecdysone hormonal cascade in *Drosophila* larval fat body remodeling. Specifically, I hypothesize that ßFTZ-F1 induces *Mmp2* expression.

Investigations were carried out through relative quantification of *Mmp2* (as compared to a control gene) expression in wild type *Drosophila* fat body as compared to fat body in which *ßftz-f1* expression has been reduced. I expected reduced expression of *Mmp2* in *ßftz-f1*-reduced fat body as compared to wild type fat body. If *Mmp2* expression is indeed induced by *ßftz-f1* expression, a reduction in *ßftz-f1* expression will result in a corresponding reduction in *Mmp2* expression. Findings demonstrated a reduction in *Mmp2* expression in *ßftz-f1*-reduced fat body aged 10 hours after puparium formation (APF). These results are consistent with the hypothesis that *Mmp2* expression is induced by *ßftz-f1* expression. Findings also demonstrated an increase in Mmp2 expression in *ßftz-f1*-reuced fat body aged 8 and 12 hours APF. These results are counter to the hypothesis. Because only one trial has been done, these results are highly preliminary.

INTRODUCTION

Tissue Remodeling in Humans

Tissue remodeling plays an important role in both normal and disease driven functions in the human body (Page-McCaw et al., 2007). It is characterized by a breakdown of extracellular matrix (ECM) allowing cells to dissociate and detach from one another and move freely throughout the body (Woessner 1991). A cell's ECM is a part of its microenvironment, and is made up of specific macromolecules organized in a network providing distinct chemical and physical properties (Lu et al., 2012, Lu et al., 2011). The ECM is a dynamic structure that is continually remodeled as various components are added or removed from the matrix (Lu et al., 2011). Tissue remodeling is necessary in many healthy mammalian functions including bone remodeling, embryonic development, and wound healing (Lu et al., 2011, Woessner, 1991). In the context of wound healing, tissue remodeling is responsible for the breakdown of damaged cells' ECM so the cells can be removed from the wound site (Stevens and Page-McCaw, 2012). Tissue remodeling also breaks down the ECM of healthy cells surrounding the wound's edge making it possible for new, healthy tissue to integrate with the surrounding cells as it fills in and repairs the wound (Stevens and Page-McCaw, 2012).

ECM dynamics, such as tissue remodeling, are a medically important area of study due to their roles in human diseases such as joint destruction leading to

rheumatoid arthritis, osteoarthritis, and cancer (Woessner, 1991, Lu et al., 2011). Tissue remodeling contributes to cancer in multiple ways. A flaw in tissue remodeling regulation can lead to uncontrolled cell proliferation leading to tumor formation (Lu et al., 2011). Most notably, tissue remodeling is believed to contribute to the metastatic activities of cancer by degrading tumor cell ECM allowing the cells to dissociate, move throughout the body, and spread the disease (Hyun and Parks, 2007). The cell dissociation action of tissue remodeling is made possible by Matrix Metalloproteinases or MMPs – which are an important area of study as a possible cancer-prevention therapy with the hope of inhibiting MMP activity, thus inhibiting the metastatic activities of cancer (Hyun and Parks, 2007).

MMPs

MMPs are zinc-dependent endopeptidases, or proteases, that degrade ECM by degrading collagen fibers and proteoglycans, and cleaving ECM proteins and peptide bonds (Woessner, 1991, Page-McCaw et al., 2007). *Mmp*s are transcribed as inactive pro-enzymes as a caution protecting against the potential dangerous actions of proteases (Gialeli et al., 2010, Hyun-Jeong and Parks, 2007). This initial transcription in an inactive state, and subsequent activation of the enzyme, is made possible by the multi-domain design of the MMP enzyme family (Kessenrock et al., 2010). There are three key domains that classify an enzyme as an MMP: the catalytic domain, the pro-peptide domain, and the hemopexin-like

domain (Kessenrock et al., 2010, Page-McCaw et al., 2007). The catalytic domain is responsible for performing the protein's actions, such as cleaving ECM proteins (Page-McCaw et al., 2007). The pro-peptide domain is located at the amino terminus of the protein, and acts as a self-inhibitor, blocking protein activation (Lu et al., 2011). The pro-peptide domain is responsible for rendering the protein inactive upon first translation (Lu et al., 2011). The hemopexin-like domain is located at the carboxyl terminus of the protein, facilitates interactions with other proteins, and is connected to the catalytic domain via a flexible hinge region of the protein (see figure 1) (Lu et al., 2011, Kessenrock et al., 2010).

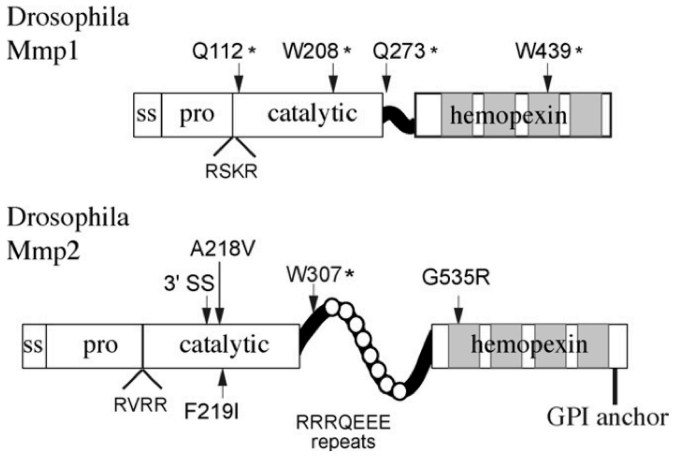

Figure 1. MMP protein domains. The pro-peptide domain, located near the amino terminus of the protein, is responsible for keeping the enzyme in an inactivated state until the appropriate activation time. The catalytic domain, located in the center of the protein, is responsible for enzymatic activity. The hemopexin-like domain, at the carboxyl terminus of the protein, and connected to the rest by a flexible hinge region, is responsible for protein-protein, or protein-cell interactions. Image from Page-McCaw (2008)

To enable MMP enzymatic activity, the protein must be activated at the pro-peptide domain, accomplished via the cysteine switch. The pro-peptide

domain maintains the MMP in an enzymatically inactive state by binding one of its cysteine residues to one of the zinc ions located in the same protein's catalytic domain. To activate the protein, the cysteine residue of the pro-peptide domain must be removed from the zinc ion of the catalytic domain. The cysteine switch can be accomplished either through a chemical modification of the residue itself thereby disrupting its interaction with the zinc ion, or by complete removal of the pro-peptide domain containing the blockading cysteine residue. Initial translation of *Mmps* as inactive enzymes requiring activation is one of many regulatory mechanisms controlling MMP activity (Kessenrock et al., 2010).

Another regulatory mechanism is the use of protease inhibitors (Kessenrock et al., 2010). In the case of MMPs, protease inhibitors aid in the regulation of the cysteine switch necessary for MMP activation (Kessenrock et al., 2010). Many proteinase inhibitors are produced in the liver and released into the blood stream maintaining generally low levels of *Mmp* expression in all resting cells (Kessenrock et al., 2010, Coussens et al., 2002). One group of protease inhibitors specific to MMPs is tissue inhibitors of metalloproteinases (TIMPs). When present at low concentrations, TIMPs help facilitate the cysteine switch, activating MMPs. At high concentrations however, as it is found under normal circumstances, TIMPs inhibit MMP activation by preventing the cysteine switch (Caterina et al., 2000).

MMP actions exhibit specific temporal and spacial expression (Lu et al., 2011). MMPs are only expressed at high concentrations during periods of tissue

remodeling such as during an inflammatory response or as an aspect of wound healing, and are confined to specific areas such as certain cells' ECM (Kessenrock et al., 2010). When expressed, not only can MMPs be confined to specific areas of the body, but also to specific spacial regions of the excreting cell's ECM (Lu et al., 2011). Tissue remodeling can create tracks of bundled collagen fibers for the excreting cells to travel along to reach specific destinations – this is made possible by highly specific *Mmp* special expression (Lu et al., 2011).

These strict regulatory functions are put in place to prevent *Mmp* expression in incorrect locations, at incorrect times, or in improper concentrations, which can lead to devastating human diseases, such as cancer (Lu et al., 2011). Due to the potential dangers of MMP actions, and the possible detrimental effects of deregulated or excessive MMPs, a large amount of energy is allocated to their regulation (Kessenrock et al., 2010).

MMPs in Human Health

Through tissue remodeling, MMPs are involved in many developmental and day-to-day processes in the human body, including organ development, inflammatory response, and wound healing (Kessenrock et al., 2010). MMPs aid in wound healing by degrading ECM connections between injured cells so the cells can be removed from the wound site, and loosening the ECM of cells surrounding the injured site creating space for uninjured cells to proliferate into

the wound site, and for new healthy tissues to integrate into the surrounding cells as the wound heals (Coussens et al., 2002).

In cancer metastasis, MMPs degrade ECM connections between tumor cells, allowing them to dissociate and detach, freeing them to migrate through the circulatory system (Coussens et al., 2002). Eventually, the migrating tumor cells will exit the vasculature in a new environment, infecting other areas of the body leading to new tumor sites, and the spread of the disease (Coussens et al., 2002). Additionally, human cancers often display unregulated expression of various ECM-related enzymes, often manifested as an over-expression of MMPs by cancerous cells (Lu et al., 2011). Cancerous cells have also been shown to have porous and "leaky" basement membranes in their ECM facilitating further metastases (Lu et al., 2011). MMPs can either be fully secreted outside of the cell, or partially secreted, remaining anchored into the cell membrane through a trans-membrane region of the protein (Hyun-Jeong and Parks, 2007). Those MMPs that are anchored to the cell membrane in this way are often specific to degrading ECM basement membrane (Stevens and Page-McCaw, 2012). Identifying MMPs as a key player in cancer metastasis has opened the door for research into *Mmp* inhibitors as a means of combating the spread of cancer (Gialeli et al., 2011).

Knowledge of the role of MMPs in cancer metastasis has been widely accepted for many years. Since this discovery, MMPs have become a target for developing new cancer therapy treatments (Kessenrock et al., 2010). Many

treatments have seen successful results in stage II trials with animal subjects, most commonly mice (Kessenrock et al., 2010). Level III clinical trials on human subjects however, have rarely demonstrated such promising results (Kessenrock et al., 2010). There are many possible reasons for this inconsistency. The most likely reason being that treatments on animal subjects can be carried out in the early stages of the disease while level III clinical trials, working with human subjects, can only be tested on patients who have progressed much further through the stages of the disease (Kessenrock et al., 2010). MMPs facilitate the spread of cancerous cells throughout the body, so would presumably not have an effect on tumors that have already established themselves and developed (Coussens et al., 2002). MMP-targeting treatments are most likely to have a preventative rather than a recovery effect, therefore tests on patients suffering from advanced stages of cancer are unlikely to experience a reduction in tumor size or number, as cancer treatment success is usually measured in clinical trials (Kessenrock et al., 2010).

Tissue Remodeling in Insects

Drosophila melanogaster serves as a useful model organism with which to study the specialized mechanisms regulating tissue remodeling, including the actions of MMPs (Stephenson and Metcalfe, 2013). Tissue remodeling can be studied through this model by examining the regulatory mechanisms facilitating the process of *Drosophila* larval fat body remodeling, an important aspect of the

animal's transition from larva to adult.

Many insects, including *Drosophila*, are holometabolous, having a larval and a pupal stage preceding the adult stage of the life cycle. During the pupal stage of the their life cycle, these insects undergo metamorphosis between the larval and adult stages, during which most larval tissues are dissolved via programed cell death (Bond et al., 2011). In some cases, cell death occurs via autophagy, allowing for the absorption and subsequent reuse of the degraded larval tissue in building new adult structures (Aguila et al., 2007). Some larval tissues are needed for further development and do not undergo programed cell death (Bond, 2010). One such larval structure is the larval fat body, which is remodeled during metamorphosis rather than reabsorbed via programed cell death (Bond et al., 2011).

Drosophila melanogaster **Life Cycle**

Drosophila melanogaster have a complex life cycle consisting of larval, prepupal, pupal, and adult stages (Aguila et al., 2007). During the prepupal and pupal stages, the *Drosophila* animal undergoes metamorphosis, which includes larval fat body remodeling (Aguila et al., 2007). *Drosophila* life cycle stages progress as follows: embryo, 1st instar larva, 2nd instar larva, 3rd instar larva, prepupa, pupa, adult (See Figure 2) (Weigmann et al.. 2003). The first stage of the *Drosophila* life cycle is the embryonic stage (Campell et al., 2005). The *Drosophila* embryo begins as one large cell that contains multiple nuclei

surrounded by an eggshell (Campell et al., 2005, pg 422). This single cell undergoes many nuclear divisions and, after about 24 hours, hatches from its eggshell and develops into a first instar larva (Campell et al., 2005, pg 421-22).

After approximately 25 hours of eating and growing, the larva molts and becomes a 2nd instar larva, and after another approximate 24 hours of continued eating and growing, molts a second time and enters the 3rd larval instar (Campell et al., 2005, pg 422). During the first two larval instars, the animal lives embedded in its food source, where the egg was initially laid, continuously feeding resulting in a 200-fold increase in mass (Aguila et al., 2007). Much of the nutrients acquired during this period of continuous feeding are stored within the larval fat body (Aguila et al., 2007).

During the third larval instar, once the larva has built up enough nutrients and mass to enter metamorphosis, it climbs out of the food source and searches for 12-24 hours for a suitable pupariation site (Aguila et al., 2007). Once finding this location, the larva ceases movement and begins puparium formation, or pupariation (Aguila et al., 2007). At this time, the animal is referred to as a zero hour prepupa (Bainbridge and Bownes, 1981). The animal remains a zero hour prepupa for a mere 15-30 minutes before completing pupariation and becoming a prepupa (Bainbridge and Bownes, 1981). Ten to twelve hours after puparium formation (APF), the *Drosophila* animal goes through the prepupal to pupal transition, marked by the eversion of the head capsule (Bond et al., 2007). During this transition period, most larval structures are dissolved, and the larval fat body

is remodeled (Bond et al., 2007). Following metamorphosis, after 3.5-4.5 days within the pupal case, the adult fly emerges, marking the final stage of the Drosophila life cycle.

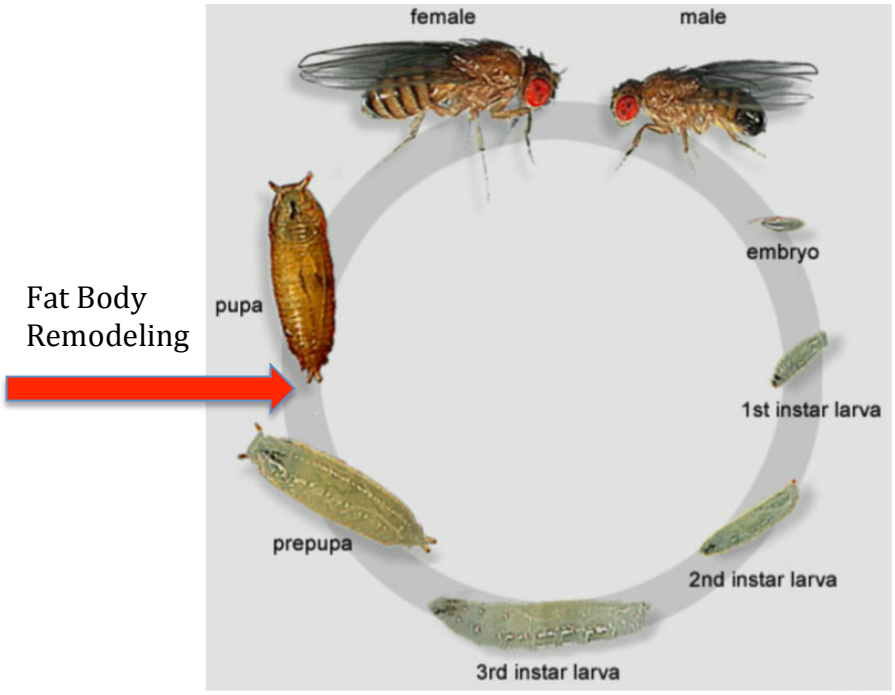

Figure 2. Life Cycle of *Drosophila melanogaster*. The *Drosophila* life cycle follows two distinct stages, the larval and the adult stage. The larval stage is split into three instars as the larva continues to grow and completes two molts of its exterior case. Once the feeding phase is complete the 3rd instar larva crawls up and out of the food in search of a location for pupariation. After settling on a pupariation location, it is considered a zero-hour prepupa, and once the prepupal case is fully formed, a prepupa. Around 10-12 hours after puparium formation (APF) the prepupa transitions into a pupa. During the transition from prepupa to pupa, larval structures are either reabsorbed through programed cell death or remodeled for continued use as occurs with the larval fat body. While inside the pupal case the adult fly develops, and after 3.5-4.5 days, the newly formed adult fly emerges from the pupal case entering the final stage of *Drosophila* development. Image from Weigmann et al. (2003)

Drosophila melanogaster Larval Fat Body

The *Drosophila* larval fat body serves as a nutrient stock that sustains the animal through metamorphosis and into the beginnings of adult life (Aguila et al.,

2007). The larval fat body plays a role in metabolism through the regulation of the release of insulin-like peptides (Géminard et al., 2009). Sensors in the larval fat body measure levels of nutrient availability and signal the brain when to release insulin-like peptides thus remotely controlling *Drosophila* metabolism (Géminard et al., 2009). Unlike many larval structures, the larval fat body is not degraded during the prepupal to pupal transition, but is remodeled and maintained through metamorphosis and into the beginnings of adult life (Aguila et al., 2007). The larval fat is absorbed via programed cell death after metamorphosis once the adult has emerged from the pupal case, extended its wings, and located a new sustaining food source (Nelliot et al., 2006).

In the young adult, the larval fat body cells provide a continued source of nutrients to the newly-eclosed adult animal until it is able to locate a new reliable external food source (Aguila et al., 2007). It takes 8 hours for the young adult's wings to expand before it can relocate to a fresh food source. Presence of the larval fat body in the young adult fly is essential for survival until this food source is located (Aguila et al., 2007). Sheets of adult fat cells replace larval fat cells once they are reabsorbed (Aguila et al., 2007). The nutrients held within adult fat cells are not as easily accessible as those of the larval fat body (Aguila et al., 2007). Newly-eclosed adult flies are almost three times as starvation resistant as older adults (Aguila et al., 2007). This is due to the continued presence of larval fat cells in the young adult fly (Aguila et al., 2007). Aguila et al. (2007) experimentally extended the lifespan of larval fat cells in the adult fly and

conducted a starvation study. Their research found that starved adults survive longer when their larval fat cells remain intact (Aguila et al., 2007).

Drosophila Larval Fat Body Remodeling

Drosophila larval fat body remodeling is characterized by a transition from single-cell thick sheets of attached polygonal fat cells to individual spherical free floating fat cells that disperse throughout the pupa (see Figure 3) (Aguila et al., 2007, Bond et al. 2011). Once dissociated, fat body cells are distributed throughout the pupal body providing nutrients to all areas of the developing pupa (Nelliot et al., 2006). This transition from sheets of attached cells to individual free-floating cells is necessary for *Drosophila* metamorphosis (Nelliot et al., 2006). A failure of fat body remodeling impedes complete development, and is lethal to the adult fly (Nelliot et al., 2006).

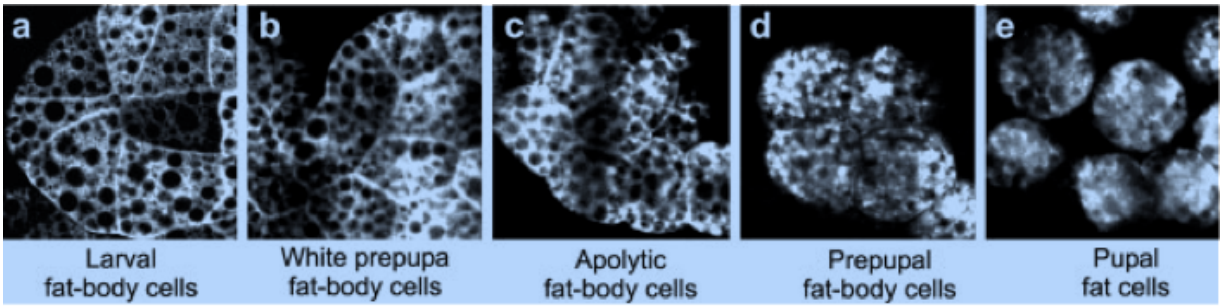

Figure 3. Dissociation of *Drosophila melanogaster* fat body cells through the process of tissue remodeling. In the larval stage fat body cells are polygonal in shape and connected in a sheet. As the larva transitions into a prepupa, fat body cells begin to shift and dissociate, becoming more spherical in shape, but remain connected to one another. During the prepupal to pupal transition, fat body cells detach from one another, now as fully formed spheres, and move individually throughout the pupa. Image from Nelliot et al., (2006).

Drosophila fat body remodeling occurs in three phases: the retraction phase, the disaggregation phase, and the detachment phase (Bond et al., 2011). The retraction phase takes place between zero and 6 hours APF, and is characterized by the retraction of the fat body from the anterior area of the prepupa (Nelliot et al., 2006). The disaggregation phase occurs between 6 and 12 hours APF, and is characterized by a change in shape of the fat body cells from flattened polygonal cells to plump spherical cells as the cells begin to lose their tight associations (Bond et al., 2011, Nelliot et al., 2006). Disaggregation of fat cells begins in the anterior region of the prepupa progresses toward the posterior end of the animal (Nelliot et al., 2006). The detachment phase occurs as part of the prepupal to pupal transition, directly following head eversion, and is the final phase of fat body remodeling (Bond et al., 2011). This phase occurs between 12 and 14 hours APF, involves full detachment of the now spherical fat cells from

one another, and movement of the newly separated and re-shaped individual fat cells into the head capsule mediated by abdominal muscular contractions (Bond et al., 2011, Nelliot et al., 2006). Any remaining fat cells that were not propelled into the head capsule are spread throughout the body of the pupa, detaching from one another in succession from anterior to posterior (Nelliot et al., 2006, Bond et al., 2011).

20-Hydroxyecdysone

Metamorphosis is regulated by expression of the ecdysteroid ecdysone and its active metabolite 20-hydroxyecdysone (from here on collectively referred to as ecdysone) (Agawa et al., 2007). Ecdysone binds to the ecdysone receptor and regulates gene expression during metamorphosis (Bond et al., 2011). The ecdysone receptor consists of two nuclear receptors: EcR (NR1H1), and USP (Ultraspiracle, NR2B4) (Kozlova and Thummel, 2003). Loss of these receptors is lethal to the animal, much in the way that a loss of ecdysone is lethal, providing evidence for the ecdysone receptor as a necessary part of successful ecdysone signaling (Kozlova and Thummel, 2003). Ecdysone –mediated control of developmental events is carried out via transcriptional cascades specific to certain tissues and processes (Bond et al., 2011).

Ecdysone is necessary for *Drosophila* larval fat body remodeling (Bond et al., 2011). Loss of ecdysone results in unsuccessful remodeling characterized by groups of non-dissociated, flat cells (Bond et al., 2011). These results

demonstrate that ecdysone is required for the second and third phases of *Drosophila* fat body remodeling: the disaggregation phase, and the detachment phase (Bond et al., 2011).

The temporally specific patterns of gene expression that regulate *Drosophila* metamorphosis are controlled in part by the rising and falling of the ecdysone titer (Woodard et al., 1994). Rises in the ecdysone titer lead to increased binding of the hormone to ecdysone receptors, inducing the transcription of certain genes triggering transcriptional cascades (Bond et al., 2011). During the early stages of metamorphosis, there are two major rises in ecdysone titer, also known as pulses: the late-larval pulse and the prepupal pulse (Nelliot et al., 2006). The late-larval ecdysone pulse occurs late in the third larval instar and triggers puparium formation, marking the beginning of the prepupal stage (Nelliot et al., 2006). The prepupal ecdysone pulse occurs approximately 10-12 hours APF, triggering the prepupal to pupal transition, and fat body remodeling (Nelliot et al., 2006). Each ecdysone pulse induces the transcription of a group of regulatory "early genes" which encode proteins that in turn induce transcription of downstream "late genes" (Agawa et al., 2007). Between the late larval and prepupal ecdysone pulses is a period of low ecdysone titer referred to as the "mid-prepupal" period (Woodard et al., 1994). Genes transcribed during this period are referred to as the mid-prepupal genes (Yamada et al., 2000). There are multiple mid-prepupal genes expressed at this time during development (3-8 hours APF), following the raise and subsequent lowering of the ecdysone

hormone titer (Woodard et al., 1994). The mid-prepupal gene of importance to this study is *ßftz-f1*.

ßftz-f1

One notable mid-prepupal gene involved in *Drosophila* development is *ßftz-f1*. The fushi tarazu factor-1 *(ftz-f1)* gene codes for two protein isoforms, α and β, which share a common C terminus, but differ in their distinct N termini (Broadus et al., 1999). The isoform of concern in *Drosophila* metamorphosis is the β isoform: ßFTZ-F1. βFTZ-F1 is an orphan nuclear hormone receptor (a receptor with no known ligand that responds to changes in hormonal concentrations) that plays a key role in modulating the actions of ecdysone in *Drosophila* metamorphosis, including fat body remodeling (Bond et al., 2011). Research carried out by Woodard et al., (1994) identified *ßftz-f1* as a key factor in characterizing the transcriptional response to the prepupal ecdysone pulse in *Drosophila* development.

The *ßftz-f1* gene is expressed throughout the animal at multiple, but specific, points during development, all following, but not simultaneous to a rise in the ecdysone titer (Agawa et al., 2007). This expression pattern is regulated by ecdysone, as well as by *ßftz-f1* itself (Woodard et al., 1994). Woodard et al. (1994) demonstrated that *ßftz-f1* is both self-repressed, and repressed by ecdysone making its expression both brief and specific. *ßftz-f1* repression by ecdysone was demonstrated through the ectopic addition of ecdysone blocking *ßftz-f1*

transcription, as well as through the removal of ecdysone increasing *ßftz-f1* expression (Woodard et al., 1994). This connection has since been demonstrated as mediated by dBlimp-1, a key aspect of this study's experimental design (Akagi and Ueda, 2011). *ßftz-f1* expression periods include: just before each larval molt, and during the mid-prepupal period of metamorphosis between the late-larval and prepupal ecdysone pulses (Broadus et al., 1999). This study focused on the downstream effects of *ßftz-f1* expression during the mid-prepupal period.

The *ßftz-f1* gene regulates many events involved in metamorphosis, including leg and wing extension, larval salivary gland programmed cell death, and larval fat body remodeling (Fortier et al., 2003). Evidence for *ßftz-f1* as a regulator of fat body remodeling lies in the simultaneous occurrence of fat body remodeling and other metamorphic actions known to be regulated by *ßftz-f1,* such as the muscle contractions moving the mid-abdominal gas bubble out of the pupal body and into the anterior space between the body and the cuticle making room for head eversion, also caused by the same muscular contractions (Fortier et al., 2003).

ßFTZ-F1 as a Competence Factor

While there are many genes transcribed during the mid-prepupal period, *ßftz-f1* is the only mid-prepupal gene that has been identified as necessary for a successful response to the prepupal ecdysone pulse (Akagi and Ueda, 2011). The *ßftz-f1* gene is a regulatory mid-prepupal gene whose product, ßFTZ-F1, is

thought to act as a competence factor regulating temporally specific responses to changes in the ecdysone titer (Broadus et al., 1999). The actions of ßFTZ-F1 as a competence factor refers to its rendering certain target genes available for transcription in response to changes in the ecdysone titer, when they were not previously competent to respond to the same stimulus (Woodard et al., 1994).

For an identical stimulus to induce two separate responses, as occurs with the late-larval and prepupal ecdysone pulses in *Drosophila* metamorphosis, there must be an alteration in the regulatory mechanisms of the affected genes occurring in between these two pulses (Woodard et al., 1994). *ßftz-f1* expression during the mid-prepupal period confers competence to certain genes, providing them with the ability to respond to the prepupal ecdysone pulse (Woodard et al., 1994). *E93* is an example of one of these target genes (Broadus et al., 1999). *E93* requires βFTZ-F1 for successful transcription in response to the prepupal ecdysone pulse (Broadus et al., 1999). ßFTZ-F1 also confers competence to *BR-C, E74A,* and *E75A*, enhancing their expression response to ecdysone (Broadus et al., 1999). Evidence from studies such as those carried out by Broadus et al. (1999), Woodard et al. (1994), and Bond et al. (2011) suggest that ßFTZ-F1 provides the necessary alterations to these genes, and others, needed to respond to changes in the ecdysone titer.

Research conducted by Broadus et al., (1999) demonstrated that *ßftz-f1* mutants respond normally to the late-larval ecdysone pulse but display largely altered responses to the prepupal ecdysone pulse. Research carried out by

Woodard et al. (1994) investigated *ßftz-f1* as a competence factor aiding in stage-specific responses to ecdysone. Woodard et al. (1994) ectopically expressed *ßftz-f1* just before the late-larval ecdysone pulse, leading to increased levels of mRNA from genes normally only expressed following the prepupal ecdysone pulse, following *ßftz-f1* expression such as E93. Bond et al. (2011) provided further evidence for *ßftz-f1* as a regulator of fat body remodeling by demonstrating that *ßftz-f1* is both necessary and sufficient for *Drosophila* larval fat body remodeling.

These results provide evidence for *ßftz-f1* as a competence factor, rendering certain genes responsive to the prepupal ecdysone pulse, carrying out its actions during the mid-prepupal period of *Drosophila* development. Larval fat body remodeling occurs in response to the prepupal ecdysone pulse, and is not induced in response to the late-larval pulse. Those genes responsible for *Drosophila* fat body remodeling may be included in this group of target genes acquiring competence from ßFTZ-F1 during the mid-prepupal period. Premature expression of *ßftz-f1* induces premature fat body remodeling, however in the absence of ecdysone complete fat body remodeling does not take place (Bond et al., 2011). Genes involved in the final stages of fat body remodeling cannot respond to the prepupal ecdysone pulse without the actions of ßFTZ-F1, nor will those genes be transcribed without the actions of ecdysone (Bond et al., 2011). This possibility is supported by Bond et al (2011) identifying *Mmp2* (a gene involved in the cell dissociation aspect of fat body remodeling) as a possible

target of the ecdysone signaling cascade, inducing fat body remodeling via ßFTZ-F1 regulatory actions.

ßftz-f1 Regulation by dBlimp-1

ßftz-f1 expression is regulated by ecdysone and the transcription factors DHR3, and dBlimp-1 (Agawa et al., 2007). DHR3 induces *ßftz-f1* expression, while dBlimp-1 blocks *ßftz-f1* transcription (White et al., 1997). Most pertinent for the purposes of this study, is the transcription factor dBlimp-1. dBlimp-1 is a homologue of the mammalian B lymphocyte-induced maturation protein-1 (Bond et al., 2011). It is an ecdysone-induced, rapidly degraded transcriptional repressor protein that represses *ßftz-f1* transcription (Bond et al., 2011). *dBlimp-1* expression is induced by the rises in the ecdysone titer, and is the mechanism by which ecdysone represses *ßftz-f1* expression (Bond et al., 2011, Agawa et al., 2007). dBlimp-1 represses *ßftz-f1*expression by binding directly to the *ßftz-f1* promoter, blocking access to its promotion site, and therefore blocking its transcription (Agawa et al., 2007).

The late larval ecdysone pulse induces both *DHR3* and *dBlimp-1* expression, but dBlimp-1 is more rapidly degraded making its expression temporally reflective of the rise in the ecdysone titer (White et al., 1997). As the ecdysone titer lowers, dBlimp-1 degrades and the DHR3 still present induces *ßftz-f1* expression, now that its promotion site is no longer blocked by dBlimp-1 (White et al., 1997). Previous research in the Woodard lab has demonstrated that

flies over-expressing *dBlimp-1* in the larval fat body display delayed and reduced expression of *βftz-f1* in the same larval structure past the point at which its expression is relevant (see figure 4) (Perez, 2014). If *βftz-f1* expression is delayed past the time frame during which it would normally confer competence to its downstream targets, no matter how high *βftz-f1* expression is following this window of time, it will be unable to complete its actions as a competence factor – its downstream targets will remain unable to respond to changes in the ecdysone titer. These findings provide evidence for dBlimp-1 as a transcriptional repressor of *βftz-f1* (Perez, 2014).

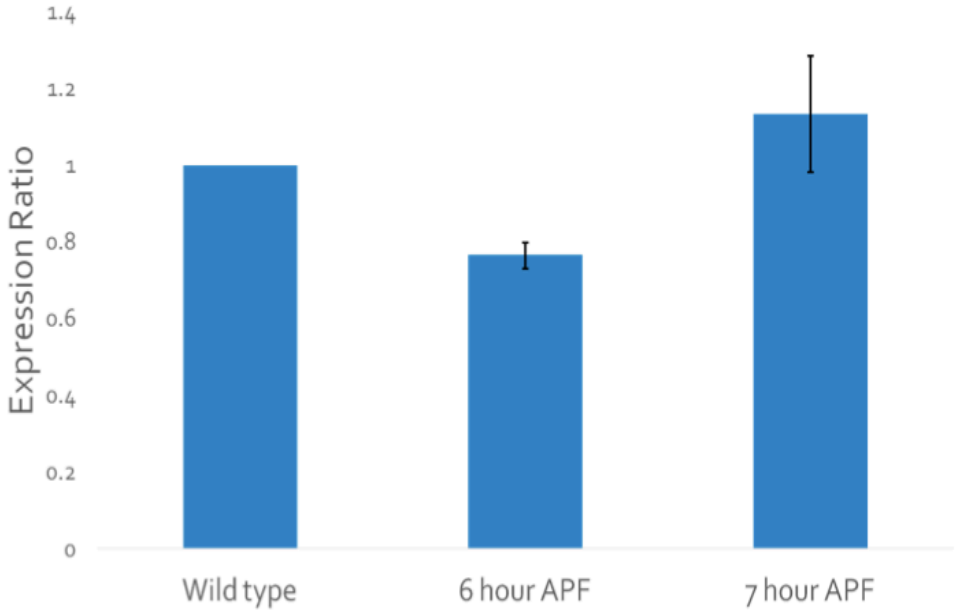

Figure 4. *ßftz-f1* expression ratios in *Drosophila* larval fat body acquired from qPCR experiments. Wild type expression ratio is noted as one. Comparisons are of *ßftz-f1* expression levels in *Drosophila* fat body over-expressing *dBlimp-1* at 6, and 7 hours APF. The 6 hour APF expression ratio, a value less than one, represents under-expression of *ßftz-f1* in fat body over-expressing *dBlimp-1* in comparison to wild type expression. The 7 hour APF expression ratio, a value greater than one, represents over-expression of *ßftz-f1* in fat body over-expressing *dBlimp-1* at this time. These results demonstrate a reduction/delay in *ßftz-f1* expression in the larval fat body in flies over-expressing *dBlimp-1*. This delay will disrupt the pattern of *ßftz-f1* expression in the larval fat body, thereby disrupting ßFTZ-F1's ability to confer competence to its downstream targets during the mid-prepupal period. Image from Perez, (2014).

dBlimp-1 expression is induced by periods of high ecdysone titer. *ßftz-f1* expression is repressed when dBlimp-1 is present (Akagi and Ueda, 2011). Due to the presence of dBlimp-1 during high ecdysone periods, *ßftz-f1* is only expressed during periods of low ecdysone (Akagi and Ueda, 2011). Even though its expression is stimulated by the rise in the ecdysone titer via DHR3 protein,

ßftz-f1 is not expressed until dBlimp-1 has degraded. *dBlimp-1* mRNA is rapidly degraded, and its levels will quickly decrease as the ecdysone titer lowers leading to *ßftz-f1* expression directly following periods of high ecdysone titer induced by DHR3 (White et al., 1997). This phenomenon is responsible for the isolation of *ßftz-f1* expression to the mid-prepupal period, following the late-larval ecdysone pulse (Akagi and Ueda, 2011).

In reference to this particular study, it is important to draw attention to the repression of *ßftz-f1* expression by dBlimp-1 during the late-larval ecdysone pulse thus isolating *ßftz-f1* to the mid-prepupal period. The action of dBlimp-1 as a repressor of *ßftz-f1* makes possible the temporally specific actions of βFTZ-F1 as a competence factor conferring competence specifically during the mid-prepupal period to genes intended for unique response to the prepupal ecdysone pulse (Akagi and Ueda, 2011). The study design takes advantage of the repressive actions of dBlimp-1 on *ßftz-f1* expression (see Figures 5 and 6).

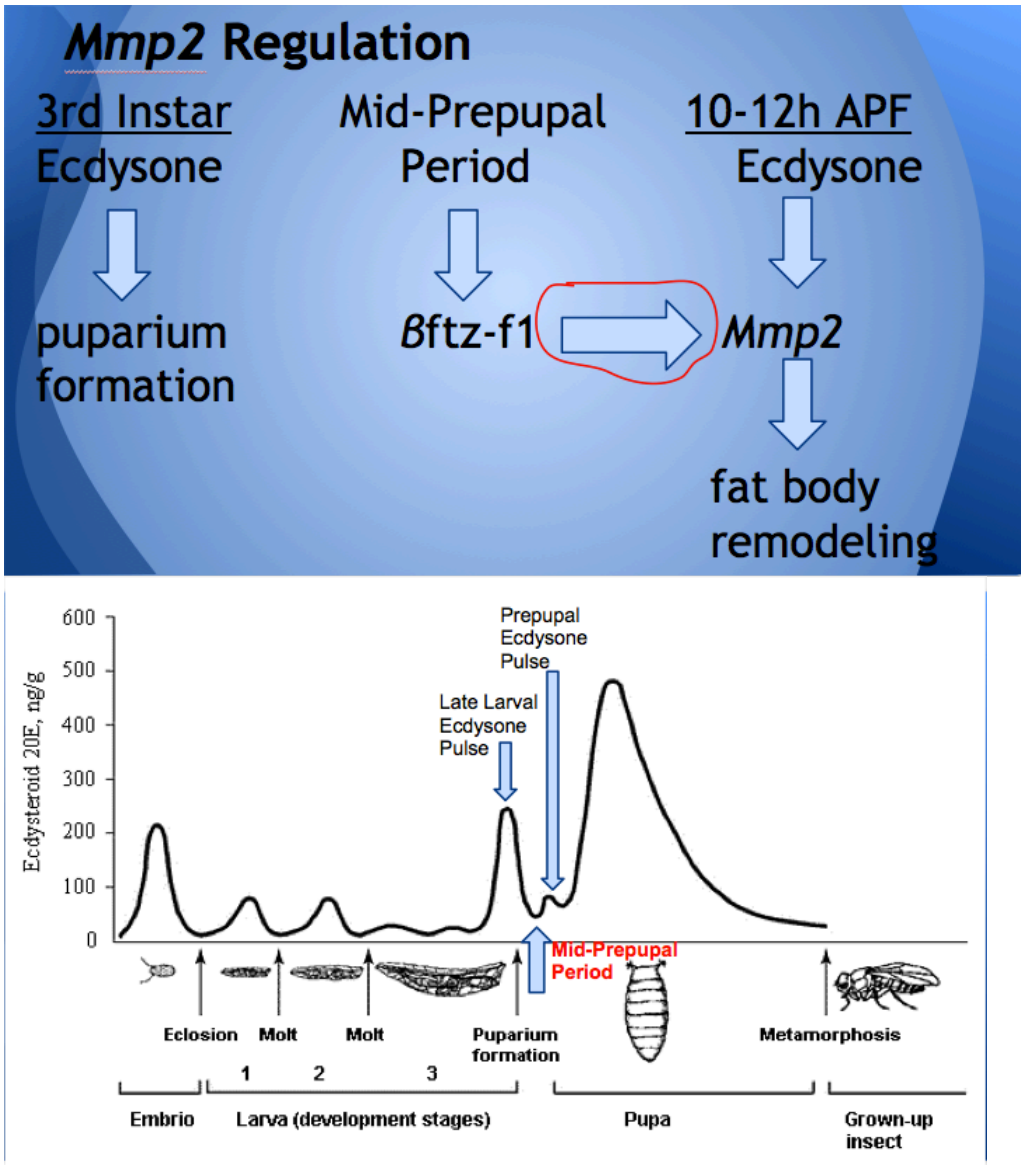

Figure 5. Hormonal regulation of *Drosophila* fat body remodeling through an ecdysone-induced protein cascade. A transcriptional cascade beginning with the late-larval ecdysone pulse regulates the temporally specific expression of *Mmp2* and subsequent fat body remodeling. During the late-larval ecdysone pulse, dBlimp-1 (also under ecdysone regulation) is expressed and inhibits *βftz-f1* expression during this ecdysone pulse. Before the pre-pupal ecdysone pulse, during the mid-prepupal period, DHR3, induced by the late-larvl ecdysone pulse, stimulates *βftz-f1* transcription in the absence of dBlimp-1. I hypothesize that in this mid-prepupal period *βftz-f1 confers* competence to *MMP2* making it available for transcription in response to the pre-pupal ecdysone pulse. Image from Timofeev, (2008).

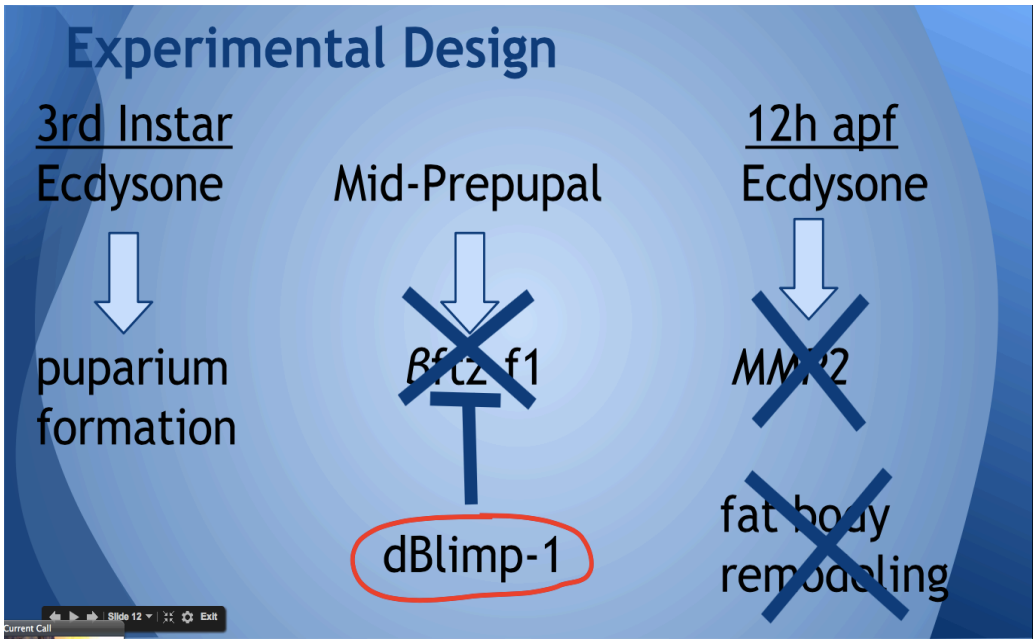

Figure 6. Experimental design demonstrating anticipated results of this study. The study uses the repressive actions of dBlimp-1 to repress *ßftz-f1* expression in the larval fat body. If *Mmp2* requires competence provided by ßFTZ-F1 to respond to the pre-pupal ecdysone pulse, a reduction or delay of *βftz-f1* will subsequently lead to a reduction in *Mmp2* expression and therefore a loss of fat body remodeling.

While *βftz-f1* has been identified as a regulator of larval fat body remodeling, other genes are required for carrying out the physical mechanisms necessary for remodeling. A key aspect of larval fat body remodeling is the disassociation of the fat body cells into individual free-floating cells. The mechanism used to separate fat cells from one another is the MMP Matrix metalloproteinase 2 (MMP2) (Qiangpiang et al., 2014). MMP2 is thought to play a vital role in larval fat body remodeling by cleaving the ECM proteins holding the fat cells together in one single sheet allowing the cells to dissociate, detach, and disperse throughout the pupa (Bond et al., 2011). In *Mmp2* mutant flies, the larval fat body fails to dissociate (Bond et al., 2011). In addition, premature

expression of *Mmp2* results in premature fat body remodeling and death of the animal (Bond et al., 2011).

MMPs in *Drosophila melanogaster*

MMPs are classified by their three specific protein domains, and have a similar genetic make-up. These similarities in the family suggest that all MMPs are derived from a common ancestor (Hyun-Jeong and Parks, 2007). There are as many as 25 MMPs in vertebrate animals, 24 of which are present in mammals (Hyun-Jeong and Parks, 2007). The large number of MMPs is most likely due to a need for redundancy; domain commonalities create many similar proteins capable of completing the same tasks thereby ensuring that the actions of MMPs are accomplished within the body (Hyun-Jeong and Parks, 2007). While none of the 25 mammalian MMPs are orthologs of either *Drosophila* MMP, *Drosophila* MMPs do maintain characteristic MMP structure, and carryout similar functions to mammalian MMPs – all MMPs are involved in the breakdown of ECM (Bond et al., 2011).

With 24 variations, it is challenging to study the role of *MMP*s in mammalian subjects (Page-McCaw, 2008). Biochemical redundancy is useful for accomplishing necessary tasks within an organism, however it is challenging in doing research. *Drosophila* have only two *MMP*s; *Mmp1* and *Mmp2,* providing a much simpler model (Page-McCaw, 2008, Qiangpiang et al., 2014). Both MMP1 and MMP2 are involved in *Drosophila* fat body remodeling; MMP2 however,

plays a larger role (Qiangpiang et al., 2014). MMP1 is involved in salivary gland destruction as well as fat body remodeling, and MMP2 is the primary MMP involved in larval fat body remodeling, degrading the basement membrane of *Drosophila* fat body cell ECM (Stevens and Page-McCaw, 2012). Recall that investigations into those MMPs responsible for degrading basement membrane are especially important due to the increased metastatic activity of cancer cells possessing "leaky" basement membranes (Lu et al., 2011). Using *Drosophila* as a research organism eliminates the issues of redundancy leading to compensation (inaccurate results due to more than one protein accomplishing the same task) (Page-McCaw, 2008).

Hypothesis

Fat body remodeling will not occur if ecdysone signaling is blocked – ecdysone is required for fat body remodeling. *Mmp2* requires ecdysone for expression, and is induced by the prepupal ecdysone pulse. If ecdysone expression is prevented, *Mmp2* is down-regulated in the larval fat body. *Mmp2* is necessary and sufficient to induce larval fat body remodeling; premature expression of *Mmp2* results in premature fat body remodeling. *βftz-f1* is also necessary and sufficient for larval fat body remodeling, and is expressed during the mid-prepupal period between the two metamorphic ecdysone pulses, just before the ecdysone pulse that induces both *Mmp2* expression and fat body remodeling. Premature expression of *βftz-f1* results in up-regulation of *Mmp2*

expression. Given that both *Mmp2* and *βftz-f1* are necessary and sufficient to induce larval fat body remodeling in *Drosophila*, early expression of *βftz*-f1 results in an up-regulation of *Mmp2*, and *βftz-f1* and *Mmp2* are simultaneously expressed, I hypothesize that *Mmp2* is a downstream regulatory target of *βftz-f1* and that a down-regulation of *βftz-f1* in the larval fat body will result in a down-regulation of *Mmp2* in the same (Bond et al., 2011).

More specifically, I hypothesize that ßFTZ-F1 confers competence to *Mmp2* during the mid-prepupal period rendering *Mmp2* available for transcription in response to the prepupal ecdysone pulse. *Mmp2* may either be a direct downstream target of *βftz-f1,* or an indirect downstream target of *βftz-f1*. A direct downstream target refers to *Mmp2* as an early gene of the prepupal ecdysone pulse receiving its competence directly from the actions of ßFTZ-F1 during the mid-prepupal period. An indirect target refers to *Mmp2* as a late gene target of the prepupal ecdysone pulse whose competence is gained through the actions of an early gene induced by the prepupal ecdysone pulse that acquired its transcriptional competence via the actions of ßFTZ-F1 during the mid-prepupal period.

βftz-f1-reduced flies are expected to display reduced *Mmp2* expression in the larval fat body. The hypothesis is that a reduced amount of ßFTZ-F1 in the larval fat body will not fully confer competence to *Mmp2*. If not competent, *Mmp2* will not respond to the prepupal ecdysone pulse (Bond et al., 2011). If not transcribed in response to the prepupal ecdysone pulse, MMP2 will not be present

in the larval fat body during the prepupal to pupal transition to break down the ECM of fat body cells. Without ECM breakdown, the second and third stages (disaggregation and detachment) of larval fat body remodeling will not be completed successfully and fat body remodeling will not complete.

MATERIALS AND METHODS

Experimental Design

The hypothesis was tested via a comparison of *Mmp2* mRNA transcripts expressed in the larval fat body at the time of larval fat body remodeling in wild-type control *Drosophila* and an experimental genotype of *ßftz-f1*-reduced *Drosophila*. The *ßftz-f1*-reduced *Drosophila* genotype will exhibit a reduction of *ßftz-f1* expression only in the larval fat body, as a full *ßftz-f1* mutant would not survive embryogenesis (Bond et al., 2011). This *ßftz-f1*-reduced *Drosophila* strain was developed by over-expressing *dBlimp-1* in the larval fat body. Over-expressing *dBlimp-1* in the larval fat body has been shown to reduce and delay *ßftz-f1* expression past its normal temporally specific expression time (See figure 4) (Perez, 2014). Delaying *ßftz-f1* expression renders its actions as a competence factor irrelevant thus creating a *ßftz-f1*-reduced genotype.

Levels of *Mmp2* mRNA transcript present in the larval fat bodies of *ßftz-f1*-reduced, and wild type animals, were compared for samples at collected at 8, 10, and 12 hours APF. Transcript levels were measured by quantitative real time PCR reactions, measuring amounts of initial transcript present in PCR reactions through relative quantification. Results were expressed as a ratio of original *Mmp2* cDNA template, to the housekeeping gene *Actin5c* (a common transcript equally expressed in all *Drosophila* tissues at high levels) (Pfaffl, 2001).

Expected results included reduced levels of *Mmp2* mRNA transcript in *ßftz-f1*-reduced fat body (wherein *ßftz-f1* expression was reduced and delayed past its relevant expression time point presumably disrupting induction of *Mmp2* expression and subsequent fat body remodeling) as compared to control specimen. (see Figure 6).

Drosophila **Genotypes**

Three genotypes were used in this study: w^{1118}, *cg-Gal4*, and *w; UAS-dBlimp-1(XA)*. The w^{1118} flies served as the wild-type *Drosophila.* w^{1118} is a stock of white-eyed flies that is otherwise wild-type. The *cg-GAL4* and *w; UAS-dBlimp-1 (XA)* flies were crossed to create the transgenic genotype *cg-GAL4; w; UAS-dBlimp-1(XA).* This genotype displays reduced levels of *ßftz-f*1 in the larval fat body as demonstrated by previous research in the Woodard lab (see Figure 4) (Perez, 2014). *ßftz-f1*-reduced flies expressed *dBlimp-1* in the fat body only via the *UAS/Gal4* system.

UAS/GAL4 **System**

The *UAS/GAL4* system involves a cross between parental flies in which a gene, in this case *dBlimp-1,* is regulated by the *Saccharomyces cerevisiae* upstream activating sequence (*UAS*) element, and parental flies containing the *Saccharomyces cerevisiae GAL4* driver under the control of a tissue specific promoter (in this case specific to the larval fat body) (Duffy, 2002). Any gene

under *UAS* control requires a *GAL4* driver for transcription (Duffy, 2002). The resulting progeny express the gene under *UAS* control (*dBlimp-1*) only in those structures (the larval fat body) included in the expression pattern of the specific *GAL4* driver present (see Figure 7) (Duffy, 2002). In this case, the *dBlimp-1* gene under *UAS* control was transcribed according to the expression pattern of the *cg-GAL4* driver in the larval fat body.

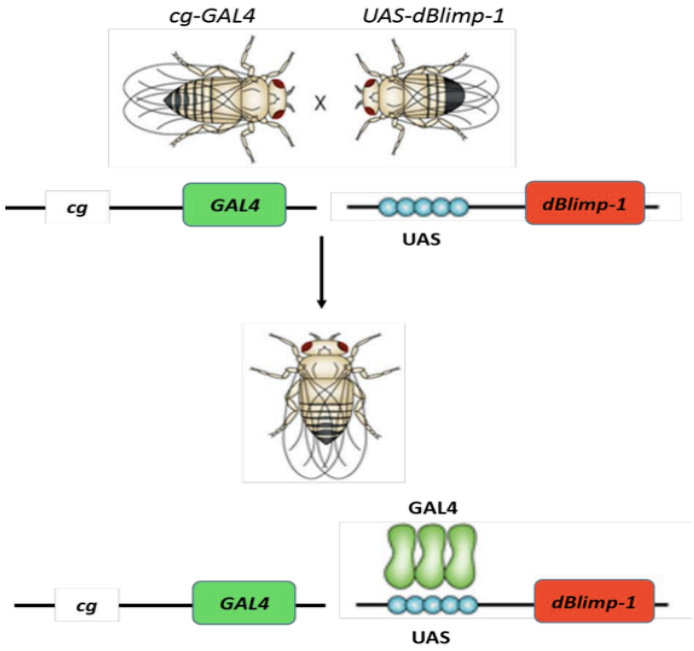

Figure 7. The *UAS/GAL4* system. In the genotype used for this study, *dBlimp-1* is under UAS control and requires a *GAL4* driver for successful transcription. *Cg-GAL4* type flies provide the driver necessary for *dBlimp-1* transcription under these conditions. The *Cg-GAL4* driver is only present in the larval fat body cells. Progeny resulting from a cross between *w; UAS-dBlimp-1(XA)* flies and *cg-GAL4* flies will therefore only express *dBlimp-1* in the larval fat body. Image from St. Johnston, (2002).

Drosophila Husbandry

All animals were housed at 25° Celsius (C) at 50% humidity in plastic bottles and vials on a standard yeast-based *Drosophila* culture medium. This medium consisted of yeast, water, agar, malt, corn syrup, cornmeal, and tegosept and propionic acid as mold inhibitors. Additional dry yeast was added to each food container before the addition of flies. Flies were transferred onto fresh medium in fresh bottles every 4-7 days in order to prevent the development of mites and maintain healthy stocks.

Virgin Collection and Experimental Crosses

In preparation for virgin fly collection, bottles with many soon-to-eclose adults were cleared of all adult flies, and cotton balls were inserted coating the top surface of the food in order to provide a clean surface for collection. Bottles were incubated at 25° C and virgins were collected within 8 hours, or at 18° C within 18 hours. Once collected, flies were sexed and kept in separate male and female viles to prevent mating until crosses were performed.

Crosses were performed in both orientations: *w; UAS-dBlimp-1(XA)* males to *cg-GAL4* females, as well as *cg-GAL4* males to *w; UAS-dBlimp-1(XA)* females (see Figure 8). Only the *w; UAS-dBlimp-1 (XA)* males to *cg-GAL4* females crosses were used to collect biological samples. This was a result of the low numbers of *w; UAS-dBlimp-1(XA)* females produced and collected during virgin collection leading to very few larva from the resulting cross.

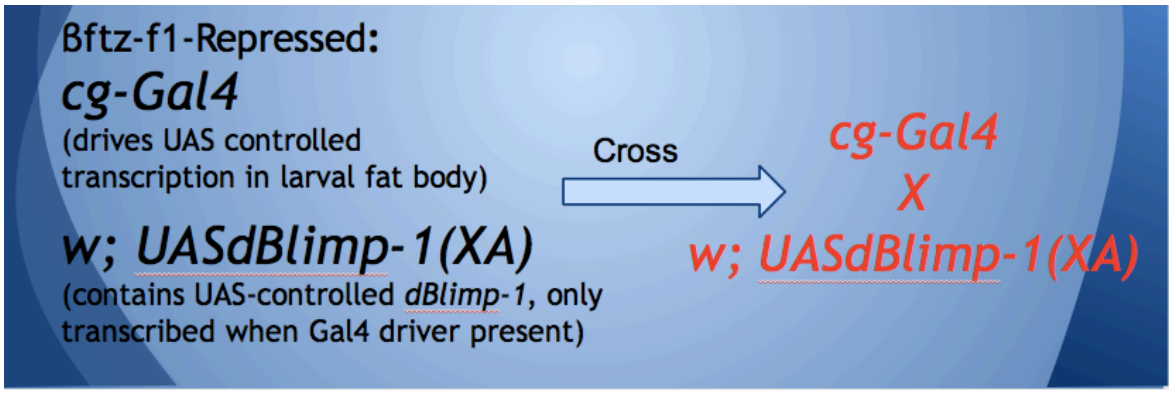

Figure 8. Development of a transgenic *Drosophila* genotype with reduced *ßftz-f1* expression in the larval fat body. *cg-Gal4* females were crossed with w; *UASdBlimp-1(XA)* males to develop a transgenic progeny over-expressing *dBlimp-1* in the larval fat body. An over expression of *dBlimp-1* in the larval fat body will result in a *ßftz-f1*-reduced strain of *Drosophila* based on previous research in the Woodard lab demonstrating a reduction of *ßftz-f1* expression in the larval fat body in flies over-expressing *dBlimp-1* in the same larval structure.

Sample Collection (Dissection of Prepupae)

Zero hour pre-pupae were collected and aged to the appropriate time point. Samples were collected at 8 hours APF, 10 hours APF, and 12 hours APF. Three biological replicates were collected at each time point – a total of three samples for each genotype at each time point. This led to a total of 18 biological samples for a total three biological replicates for each of the six unique sample types (w^{1118} at 8, 10, and 12 hours APF, and *ßftz-f1*-reduced at 8, 10, and 12 hours APF). Fat body was dissected into microfuge tubes containing 30 µl of 1x phosphate buffered saline (PBS) using 0.10mm x 0.06mm Dumostar #5 tweezers.

RNA Isolation

RNA was isolated from collected fat body samples. Following dissection, samples were homogenized in 300 µl of TRIzol reagent acquired from Life Technologies and frozen at -80° C. To complete RNA isolation, samples were thawed and transferred to phase lock gel-heavy 2 ml tubes acquired from 5 PRIME that were first pre-spun at 12,000 rpm for one minute. 60 µl of chloroform was added to the TRIzol and fat body sample and spun for 10 minutes at 12,000 rpm at 4° C. Following the spin, the RNA was separated from all other components (DNA, TRIzol, protein) by a thick gel layer. This separation was clearly visualized as a clear liquid layer of RNA on top, a middle layer of cloudy gel, and a bottom layer of pink TRIzol reagent and dissolved substances. If the separation was not successful, 60 µl of chloroform were added and the sample was re-spun. The top aqueous layer containing the RNA was then transferred to a fresh nuclease-free microfuge tube. 160 µl of isopropanol was added to the sample and mixed by inverting the tube repeatedly and set to precipitate overnight at -20° C.

The following day, the sample was centrifuged at 4° C for 20-30 minutes at 13,400 rpm. Following the spin, a small pellet was visible at the bottom of the microfuge tube. The supernatant was removed by pipet, leaving only the pellet in the tube. The pellet was washed with 500 µl of 75% ethanol and spun at 4° C for 5-10 minutes at 13,400 rpm. The pellet was still visible following the addition of ethanol. The ethanol was removed by pipet and the pellet was left to air dry for 1-

2 minutes. The pellet was then re-suspended in 5 µl of nuclease-free water, incubated for 10 minutes at 55° C to facilitate diffusion, and then vortexed, spun down, and left at room temperature for five minutes before freezing at -80° C.

DNase Treatment to Remove Contaminating DNA

RNA concentration was quantified using the Thermoscientific NanoDrop 2000c spectrophotometer to measure 1 µl of the sample. The 260/280 value, 260/230 value, absorbance curve, and overall nucleotide concentration values were examined and recorded.

Following quantification, DNase treatment was done using the Ambion DNA-free DNase treatment. DNase-I was used to remove any contaminating genomic DNA remaining in the RNA sample. Before beginning the treatment all reagents were thawed and vortexed. One µl of 10x DNase buffer, and 1 µl of rDNAse-I were added to the sample which was then incubated at 37° C for 25-30 minutes. Following incubation, 2 µl of DNase inactivation reagent were added, and the samples were incubated at room temperature for 2 minutes, during which time they were vortexed and spun down 2 times. Samples were then centrifuged at 4° C for 90 seconds at 10,000 RPM. Following the spin, the supernatant, containing the RNA, was transferred to a fresh nuclease free microcentrifuge tube using a pipet. The entire procedure was repeated using 1.5 µl of DNase buffer,- the procedure remained otherwise identical. RNA concentration was re-quantified in the same manor as before the DNase treatment. All samples

demonstrated a concentration over 200 and a 260/280 value over 1.5 following DNase treatment.

First Strand cDNA Synthesis Using Oligo (dT)

First strand cDNA synthesis was completed using the First Strand SuperScript Reverse Transcriptase System Kit for RT-PCR from Life Technologies. Master mixes were created to run four reactions at one time, two for each RNA sample. Two cDNA reactions were run for each RNA sample, the second lacked reverse transcriptase enzyme, serving as a negative control for PCR reactions. One reaction was carried out using SuperScript II RT and one using DEPC-treated water. The reaction carried out with DEPC-treated water rather than SuperScript II RT should produce no cDNA as it lacks the enzyme necessary to complete cDNA synthesis. The hope was to create one stock of successful cDNA and one stock containing no cDNA (acting as the negative control).

The first master mix contained the following reagents: 4 µl of 10 mM dNTP mix, 4 µl of Oligo(dt) primer, and 28 µl of DEPC-treated water. Two small tubes for each RNA sample were labeled with the sample name and either "RT" or "no RT" to indicate the presence or absence of SuperScript II RT. 1 µl of the appropriate RNA was added to each tube as well 9 µl of the master mix. These samples were incubated at 65° C for five minutes and then chilled on ice for one minute (see Table 1).

Table 1. Master mix 1 used for first strand cDNA synthesis.

Reagent	Volume for One Reaction (µl)
10 mM dNTP Mix	1
Oligo (dT) Primer	1
DEPC-Treated Water	7
RNA	1

While the samples were incubating a second master mix was prepared. This mix was prepared with the following reagents, added in the indicated order: 8 µl of 10x RT buffer, 16 µl of 25mM $MgCl_2$, 8 µl of 0.1 M DTT, and 4 µl of RnaseOUT. 9 µl of the second master mix were added to each of the RNA + master mix 1 tubes and they were mixed and incubated at 42° C for 2 minutes. Following incubation, 1 µl of SuperScript II RT was added to each tube labeled "RT" and 1 µl of DEPC-treated water was added to each tube labeled "no RT". All samples were then incubated at 42 degrees Celsius for 50 minutes to facilitate cDNA synthesis. Following incubation, the reaction was terminated by incubating the samples at 70°C for 15 minutes, after which the samples were chilled on ice. After chilling, the samples were spun down to collect, 1 µl of Rnase H was added, and they were incubated at 37 degrees Celsius for 20 minutes. cDNA was stored at -20 degrees Celsius (see Table 2).

Table 2. Master mix 2 used for first strand cDNA synthesis.

Reagent	Volume for One Reaction (µl)
10x RT Buffer	2
25 mM $MgCl_2$	4
0.1 M DTT	2
RNase OUT	1

Primer Design

Two sets of primers were used for this study. Those used for *Actin 5c* amplification, and those used for *Mmp2* amplification (See Table 3). *Actin 5c*, a housekeeping gene, was used as a control/reference gene. Housekeeping genes are necessary for cell survival, and are therefore guaranteed to be present in all surviving cells under any experimental conditions (Pfaffl, 2001). Previous members of the Woodard lab provided *Actin 5c* primers, and *Mmp2* primers were acquired from Integrated DNA Technologies (IDT) (Pohl, 2014).

Table 3. Forward and Reverse primer sequences for *Mmp2* and *Actin 5c.*

Gene	Primer ID	Sequence
MMP2	Forward	5'-AGCAA TCCGGAGTCTCCAGTCTTT-3'
	Reverse	5'-TGGAGCCGATTTCGTGATACAGGT-3'
Actin 5C	Forward	5′-TCTACGAGGGTTATGCCCTT-3′
	Reverse	5′-GCACAGCTTCTCCTTGA TGT-3′

Reverse Transcriptase PCR

In order to demonstrate successful cDNA synthesis of both *Mmp2* and the *Actin 5c,* reverse transcriptase polymerase chain reactions (RT-PCR) were performed for all samples. Two master mixes were prepared to prep the cDNA samples for each PCR reaction. One was prepared to amplify *Mmp2* cDNA, while the other was prepared to amplify *Actin 5c* cDNA. Each mix supplied two reactions, the "RT" cDNA as well as the "no RT." The mixes were comprised of the following reagents: 10 µl 10X PCR buffer, 6 µl 50mM $MgCl_2$, 2 µl dNTP mix, 4 µl of either *Mmp2* or *Actin 5c* forward primer, 4 µl of either *Mmp2* or *Actin 5c* reverse primer, 69.2 µl nuclease free water, and 0.8 µl *Taq* polymerase. Four smaller tubes were labeled identifying the sample name, the target gene, and "RT" or "no RT" cDNA. 2 µl of the appropriate cDNA was added to each tube along with 48 µl of the appropriate master mix (see Table 4).

Table 4. Reaction mixture for RT-PCR.

Reagent	Amount per reaction	Final concentration
10X PCR Buffer-$MgCl_2$	5µl	1X
50mM $MgCl_2$	3µl	3mM
10mM dNTPs	1µl	200nM
10µM *Mmp2* or *Actin 5c* forward primer	2µl	400nM
10µM *Mmp2* or *Actin 5c* reverse primer	2µl	400nM
cDNA	2µl	
Nuclease-free water	34.6µl	
Taq Polymerase	0.4µl	2 units
Final volume	50µl	

Prepared PCR reactions were placed into the thermocycler for 1 hour and 21 minutes and heated to the temperatures outlined in table 5. After completing 35 cycles, the PCR amplification products were visualized using Gel electrophoresis. Any remaining PCR product following gel electrophoresis was stored at -20 degrees Celsius.

Table 5. Thermocycler profile for *Mmp2* and *Actin 5c* RT-PCR amplification.

Stage	Temperature (°C)	Time	Cycle count
Denaturation	94	30 seconds	
Annealing	55	30 seconds	35 cycles
Extension	72	30 seconds	
Final Extension	72	5 minutes	1 cycle
Final Hold	4	-	

Gel Electrophoresis

Gel electrophoresis was carried out for all samples following RT-PCR amplification to visualize RT-PCR amplification success, and demonstrate the presence of the genes of interest in the cDNA RT samples. A 1.6% agarose gel consisting of 50 mL 1X TAE, 0.8 g agarose, and 5 µl ethidium bromide (to visualize DNA bands under fluorescence) was used. Additional ethedium bromide was added to completed gels to achieve greater fluoresce in images. Each gel ran in 1x TAE for 40 minutes at ~ 130 volts. A Fujifilm LAS-3000 Luminescent Image Analyzer was used to visualize bands of DNA in the gel. The band location was compared to a DNA ladder to match up the visualized band size with the appropriate base-pair length on the ladder.

Quantitative Real Time PCR (qPCR):

qPCR is a method for quantifying gene expression that measures the amount of cDNA (synthesized from mRNA) present in the initial qPCR template (Yuan et al., 2006). This method provides quantitative data representing levels of actual gene expression. This study used relative quantification to complete a comparison between the target gene, *Mmp2* and the control gene, *Actin 5c* in initial qPCR template levels to quantify *Mmp2* expression in *ßftz-f1*-reduced fat body compared to wild-type fat body. Using relative quantification accounts for the varying amounts of fat body collected in initial biological samples.

qPCR was run using the Rox SYBR Green 2.5x master mix. qPCR

measures fluorescence levels as a way of quantifying the amount of template amplification. SYBR Green binds to double stranded DNA and fluoresces, providing a tag for measuring levels of double stranded DNA present in the qPCR reaction – SYBR Green only fluoresces when bound to double stranded DNA (Pfaffl, 2001). qPCR quantifies the initial amount of cDNA present in the qPCR reaction by determining how many amplification cycles it takes for the initial template to reach the threshold amount necessary for entrance into the exponential phase of qPCR amplification. This cycle number is referred to as the Ct value – this is the value of importance in analyzing quantifiable qPCR data. Lower Ct values correspond with higher levels of initial cDNA transcript, as it will take fewer cycles to reach the threshold amount (Yuan et al., 2006). Data are analyzed as ratios representing the difference in Ct values between a target gene (*Mmp2*) and a control gene (*Actin 5c*). The point at which the double stranded DNA in the reaction reaches the threshold is measured by fluorescence level marked by SYBR Green when bound to double stranded DNA. This method is much more accurate than RT-PCR when quantifying gene expression, but still has the potential for error because SYBR green will bind to any double stranded DNA in the qPCR reaction, including any primer dimer that may be present (Yuan et al., 2006).

Primer Optimization

Primer concentrations were adapted from previous optimizations completed in the Woodard lab (See Table 6) (Papalexi, 2013). The qPCR machine in the University of Massachusetts Genomics Resource lab (used in this study) recommends qPCR reactions of 20 µl volumes. Calculations were carried out to reach the appropriate primer concentrations as outlined by Papalexi (2013) within a reaction of the specified volume.

Table 6. Optimal primer concentrations as outlined by Papelexi (2013)

Primer	Optimal Concentrations
Actin 5c (forward)	500nM
Actin 5c (reverse)	300nM
MMP2 (forward)	500nM
MMP2 (reverse)	500nM

qPCR Standard Curves and Efficiencies

The Pfaffl method for qPCR analysis was used to analyze qPCR data. This method requires including wells to generate standard curves on each qPCR plate (Pfaffl, 2001). Whole animal cDNA was synthesized from 6-7, 12 hour APF pupae. Whole animal cDNA was diluted in serial dilutions beginning with undiluted cDNA and adding nuclease-free water in successive 1:2 dilutions. Serial dilutions were achieved by adding 10 µl of undiluted cDNA to 10 µl of nuclease-free water to achieve the 1:2 cDNA dilution, adding 10 µl of the 1:2 cDNA dilution to 10 µl of nuclease-free water to achieve a 1:4 cDNA dilution,

adding 10 µl of the 1:4 cDNA dilution to 10 µl of nuclease-free water to achieve a 1:8 dilution, and adding 10 µl of the 1:8 dilution to 10 µl of nuclease-free water to achieve a 1:16 dilution. Serial dilutions of this kind were used to set standard amplification curves for both *Mmp2* and *Actin 5c* primer efficiencies. A total of 10 experimental qPCR wells were used for standard curve reactions.

Following qPCR reactions, Ct values from standard curve wells were plotted as Y values against X values of the log of each cDNA concentration acquired via Nanodrop measurements. The slope of the concentration vs Ct value lines was used to determine the corresponding primer amplification efficiencies using equation 1.

$$Efficiency = 10^{\left(-\frac{1}{slope}\right)}$$

(equation 1)

Experimental qPCR Set Up

48 additional wells were used to gather experimental data, for a total of 58 experimental wells including those used to generate standard curve data (see Appendix 1). Eight experimental qPCR wells were set up for each unique experimental sample type: 3 wells containing cDNA with *Mmp2* primers, and one *Mmp2* no RT control; 3 wells containing cDNA with *Actin 5c* primers, and one *Actin 5c* no RT control. With a total of 6 unique experimental sample types (wild type and *ßftz-f1*-reduced fat body collected at 8, 10, and 12 hours APF), as well as

the 10 plate wells used to generate standard curve data, this set up used 58 total experimental qPCR wells. Each experimental well contained 18 µl of the appropriate qPCR master mix (see tables 7 and 8) and 2 µl of the appropriate cDNA. qPCR was run following the thermocycler profile outlined in table 9.

Table 7. Reaction mixture for *Actin 5c* qPCR reactions.

Reagent	Amount for 1 Reaction
2.5X Real SYBR Green + ROX	8 µl
Actin 5c Primer (forward) 500 nM	1 µl
Actin 5c Primer (reverse) 300 nM	0.6 µl
cDNA	2 µl
Nuclease-free water	11.6 µl *

*Due to a calculation error, 11.6 µl of nuclease-free water were used in the *Actin 5c* master mix, bringing the total reaction volume to 23.2 µl rather than the intended 20 µl. In future studies, 8.4 µl of nuclease-free water should be used in the *Actin 5c* qPCR master mix when using a final reaction volume of 20 µl. This error should not have any effect on the results presented in this study. The additional 3.2 µl of nuclease-free water was included in every *Actin 5c* qPCR well, therefore all volumes, while different between *Mmp2* and *Actin 5c* wells, were consistent throughout all *Actin 5c* reactions. Due to this consistency, comparisons are still valid, as all ratios include the same factor of difference between *Mmp2* and *Actin 5c* reactions.

Table 8. Reaction mixture for *Mmp2* qPCR reactions.

Reagent	Amount for 1 Reaction
2.5X Real SYBR Green + ROX	8 µl
MMP2 Primer (forward) 500 nM	1 µl
MMP2 Primer (reverse) 500 nM	1 µl
cDNA	2 µl
Nuclease-free water	8 µl

Table 9. Thermocycler profile used in qPCR reactions.

Stage	Temperature (°C)	Time	Cycle Count
Taq Activation	95	4 minutes	1 cycle
Separation	95	15 seconds	
Annealing	55	30 seconds	40 cycles
Extension	72	30 seconds	
Dissociation			1 cycle

qPCR Data Analysis

qPCR data were analyzed using the Pfaffl method as outlined in Pfaffl (2001). This method presents two possible methods for analyzing qPCR data while taking primer efficiency into account: relative and absolute (Pfaffl, 2001). This study used the relative quantification method, using *Actin 5c* as a reference gene against which to compare the target gene *Mmp2*. Using relative quantification accounts for the varied amounts of fat body collected during initial dissections. The Pfaffl method corrects for the amplification efficiency of the primers used in qPCR reactions by incorporating those efficiencies into the equation used to determine relative expression ratios (see equation 2). Results are expressed as a ratio of the delta Ct values between *Mmp2* amplification in w^{1118} fat body and *ßftz-f1*-reduced fat body as compared to the *Actin 5c* delta Ct values between *Actin 5c* amplification in w^{1118} fat body and *ßftz-f1*-reduced fat body, while considering qPCR primer amplification efficiencies.

$$Ratio = \frac{(E_{target})^{\Delta C_T(control-experimental)}}{(E_{reference})^{\Delta C_T(control-experimental)}}$$

(equation 2)

RESULTS

Observations During Dissections

Preliminary observations made while dissecting wild-type and *ßftz-f1*-reduced fat body demonstrated a general trend. Fat body remodeling was clearly observed in all wild-type dissections at 8, 10, and 12 hours APF. Observations of fat body remodeling were defined as the visual presence of free floating spherical fat body cells. In wild-type 8 hour APF fat body dissections, fat body was generally observed as connected polygonal cells, with small amounts of free floating fat body cells. In wild-type 10 hour APF fat body dissections, fat body was observed both as connected collections of either polygonal or spherical cells in the process of remodeling, or in the form of free floating cells. In wild-type 12 hour APF fat body dissections, nearly all fat body cells were observed as free-floating spherical cells with occasional clusters of spherical cells. Overall, wild-type fat body dissections demonstrated increased levels of fat body remodeling in older prepupae and pupae.

While dissecting *ßftz-f1*-reduced fat body, remodeling was observed less often overall, and was only minimally observed in younger prepupae. In *ßftz-f1*-reduced 8 hour APF fat body dissections, fat body was almost completely attached in cell sheets; only minimal signs of remodeling were observed. In *ßftz-*

f1-reduced 10 hour APF fat body dissections, fat body still showed only minimal signs of detachments (the majority of fat cells had not begun to show sings of remodeling). Those cells that had detached, maintained a flat, polygonal shape, and had not dissociated into the characteristic round, spherical shapve observed in wild-type remodeled fat cells. In *ßftz-f1*-reduced 12 hour APF fat body dissections, fat body cells were only partially detached. Rather than complete detachment, as observed in the wild-type 12-hour APF samples, only part of fat body had dissociated and detached, remodeling into free-floating, spherical fat cells. These observations were consistent with previously published findings (Bond et al., 2011).

Visualization of PCR Products via Gel Electrophoresis

Gel electrophoresis was used to visualize RT-PCR products testing the success of PCR primers, cDNA synthesis, and gene presence. Successful PCR was achieved at all experimental time points from both w^{1118} fat body and *ßftz-f1*-reduced fat body. While PCR amplification was visible all time points, not all PCR reactions were successful in amplifying both *Actin 5c* and *Mmp2* transcript (From three biological replicates of each unique sample type, at least one visualization, but not always all, demonstrated successful amplification).

PCR amplification of 8 hour APF fat body samples was successful for both w^{1118} and *ßftz-f1*-reduced cDNA (see Figures 1 and 2). w^{1118} samples returned bright bands for both *Mmp2* and *Actin 5c* amplification (see Figure 9).

Primer dimer is visible in all loaded lanes, and a faint band is detectable in the *Actin 5c* no RT lane. The *ßftz-f1*-reduced samples produced bright bands for both *Mmp2* and *Actin 5c* amplification (see Figure 10). Small amounts of primer dimer are visible in all loaded lanes, and a very faint band is detectible in the *Actin 5c* no RT lane.

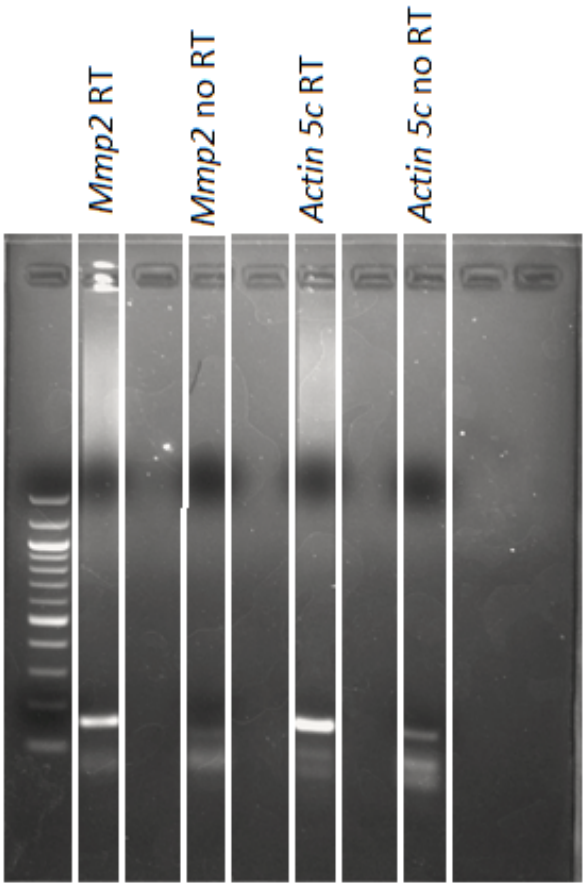

Figure 9. Image of gel electrophoresis run on RT-PCR products of cDNA synthesized from RNA of w^{1118} fat body dissected from prepupa aged 8 hours APF. The image clearly demonstrates successful RT-PCR amplification of both *Actin 5c* and *Mmp2*

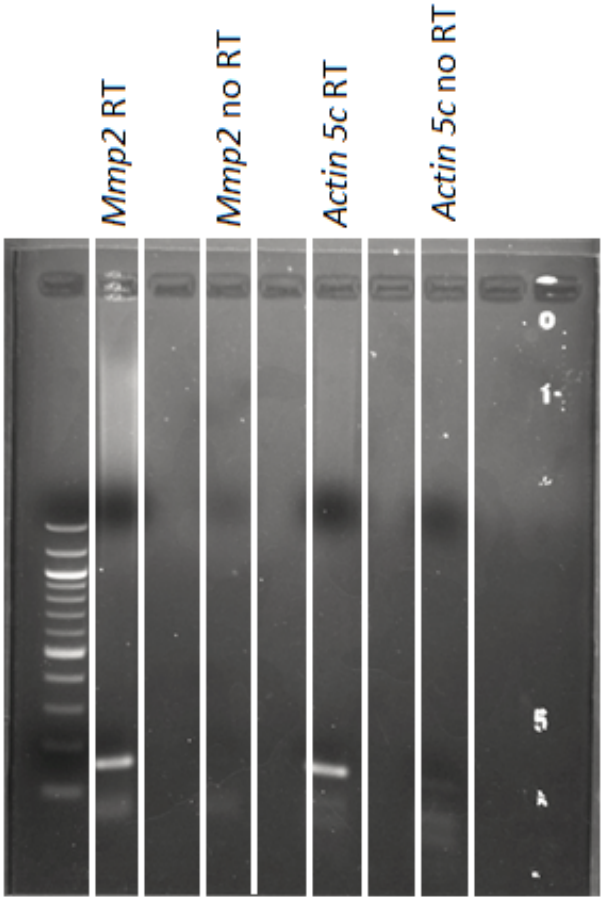

Figure 10. Image of gel electrophoresis run on RT-PCR products of cDNA synthesized from RNA of *ßftz-f1*-reduced fat body dissected from prepupa aged 8 hours APF. The image clearly demonstrates successful RT-PCR amplification of both *Actin 5c* and *Mmp2.*

PCR amplification of 10 hour APF fat body samples was successful for both w^{1118} and *ßftz-f1*-reduced cDNA. The w^{1118} samples produced a bright band in the *Actin 5c* lane, and a faint band in the *Mmp2* lane (see Figure 11). Primer dimer was faintly visible in all lanes, but no clear bands were visible in either no RT lane. The *ßftz-f1*-reduced samples produced clear bands for both *Mmp2* and

Actin 5c amplification; the *Actin 5c* band was visualized as slightly brighter (see Figure 12). Primer dimer was visible in all lanes except for the *Actin 5c* no RT lane, in which there was no evidence of amplification. A band was visible in the *Mmp2* no RT lane.

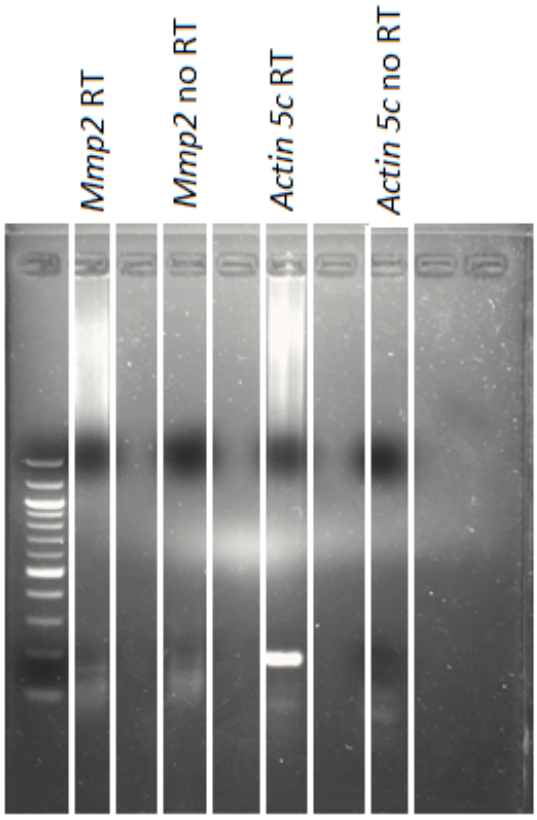

Figure 11. Image of gel electrophoresis run on RT-PCR products of cDNA synthesized from RNA of w^{1118} fat body dissected from prepupa aged 10 hours APF. The image demonstrates successful RT-PCR amplification of both *Actin 5c* and *Mmp2*. While the *Mmp2* band is faint, the slight presence of a band indicates successful *Mmp2* amplification.

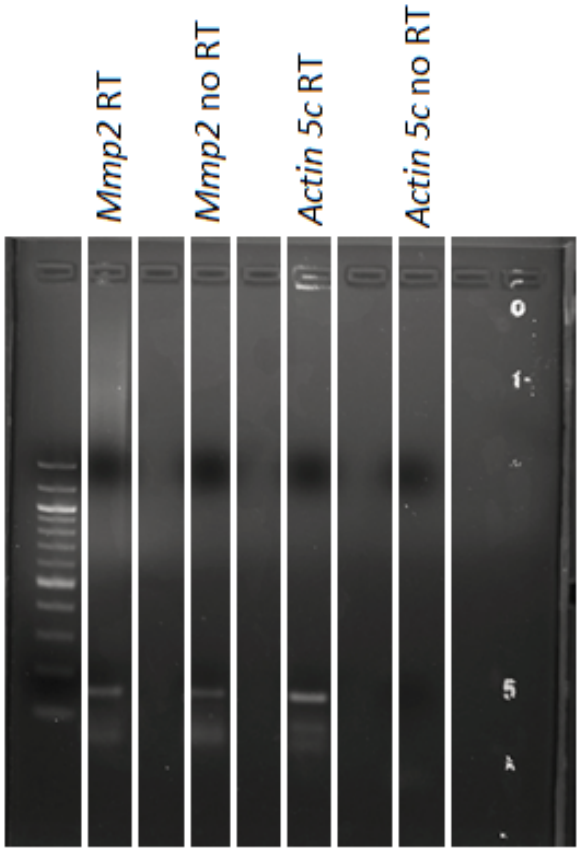

Figure 12. Image of gel electrophoresis run on RT-PCR products of cDNA synthesized from RNA of *ßftz-f1*-reduced fat body dissected from prepupa aged 10 hours APF. This image demonstrates successful RT-PCR amplification of both *Actin 5c* and *Mmp2*. While all bands are rather faint, the slight presence of a band indicates successful amplification.

PCR amplification of 12 hour APF fat body samples was successful for both w^{1118} and *ßftz-f1*-reduced cDNA. The w^{1118} samples produced clear bands for both *Mmp2* and *Actin 5c* PCR amplification; the *Actin 5c* band was slightly brighter (see Figure 13). Primer dimer was visible in all lanes, and bands were visible in both the *Mmp2* and *Actin 5c* no RT lanes. The *ßftz-f1*-reduced samples produced bands for both *Mmp2* and *Actin 5c* amplification; both bands were only

slightly fluoresced (see Figure 15). Primer dimer was visible in all used lanes, and a band was visible in the *Mmp2* no RT lane.

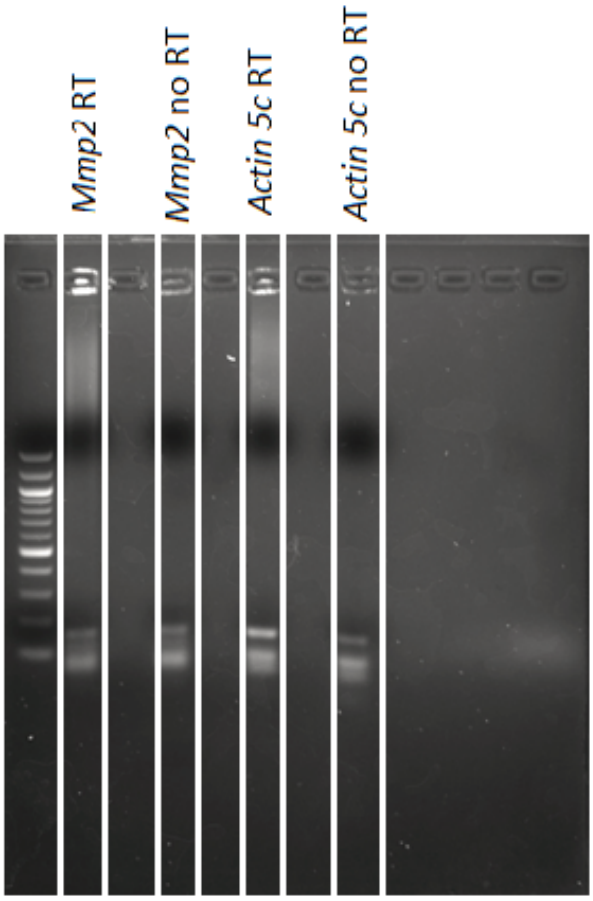

Figure 13. Image of gel electrophoresis run on RT-PCR products of cDNA synthesized from RNA of w^{1118} fat body dissected from pupa aged 12 hours APF. This image demonstrates successful RT-PCR amplification of both *Actin 5c* and *Mmp2*. While the Mmp2 band is faint, the slight presence of a band indicates successful amplification.

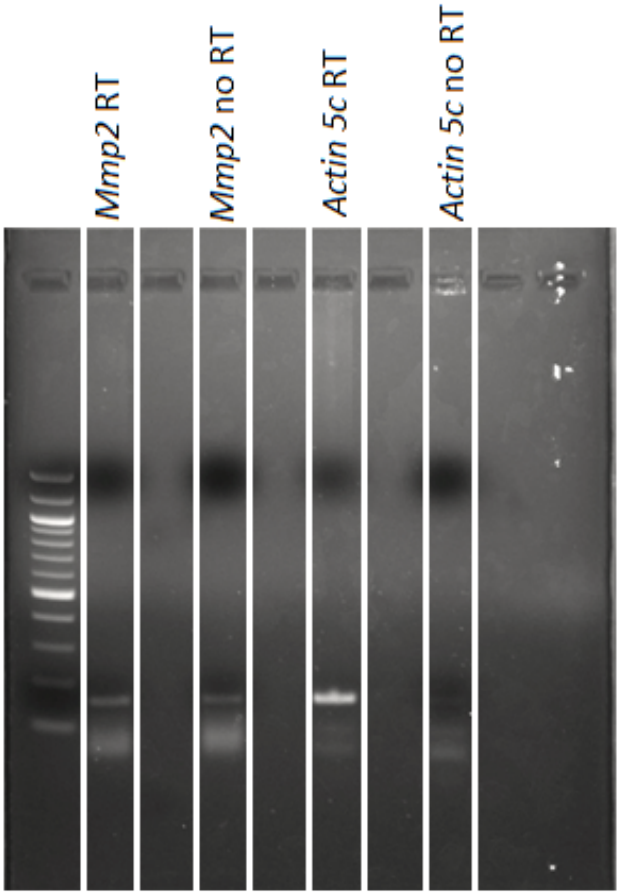

Figure 14. Image of gel electrophoresis run on RT-PCR products of cDNA synthesized from RNA of *ßftz-f1*-reduced fat body dissected from pupa aged to 12 hours APF. This image demonstrates successful RT-PCR amplification of both *Actin 5c* and *Mmp2*. While all bands are rather faint, the slight presence of a band indicates successful amplification.

Quantitative Real-Time PCR Standard Curves and Primer Efficiencies

To correct for primer efficiencies, using the Pfaffl method, standard curves were generated for *Actin 5c* and *Mmp2* template amplification using serial dilutions of cDNa synthesized from w^{1118} whole body animals aged to 12 hours

APF. As the standard curve wells were included on the same plate as all experimental wells, the curves were a valid determinant of the amplification efficiency of that particular round of qPCR. Five serial dilutions were included on the plate to generate the standard curve (1:1, 1:2, 1:4, 1:8, 1:16). Only the 1:1, 1:2, 1:4, and 1:8 dilutions were used to generate the *Actin 5c* primer standard curve. The 1:16 dilution had a multiple-peaked dissociation curve (indicating amplification and quantification of primer dimer rather than solely amplified cDNA) and was consequently removed from the analysis. The standard curve slope for *Actin 5c* was -2.8 (see Figure 15). From this slope, the efficiency of *Actin 5c* primers was found at 2.28 using equation 1.

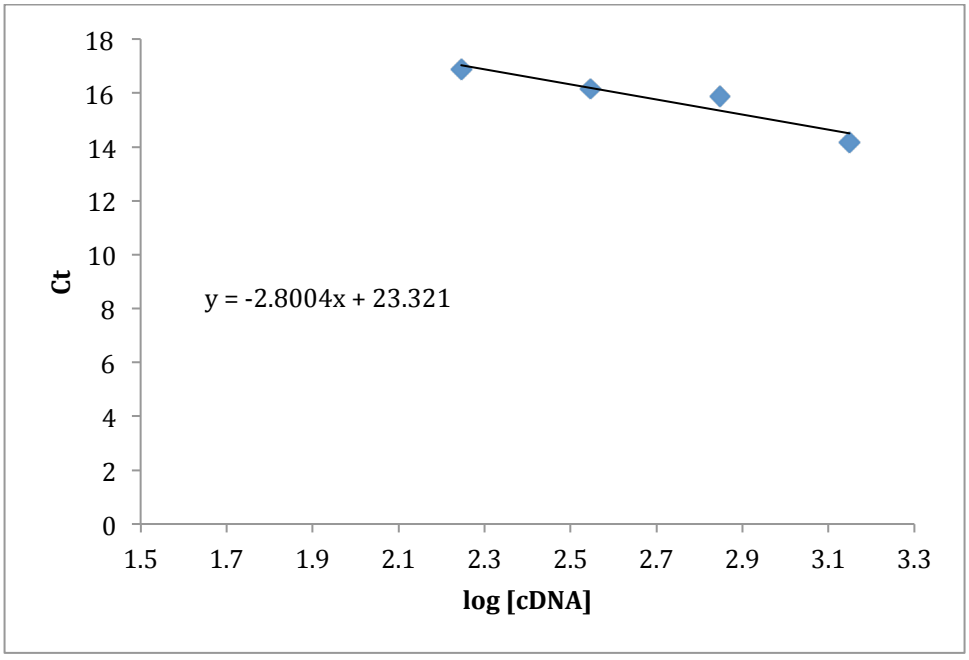

Figure 15. *Actin 5c* primer standard curve. The log of serial diluted cDNA from whole body w^{1118} animals aged 12 hours APF was plotted against DNA concentration in each serial dilution. The slope of the standard curve line was used to determine the *Actin 5c* primer amplification efficiency for the particular qPCR reaction. The slope of -2.8004 yielded an efficiency of 2.28.

Only the 1:2, 1:4, and 1:16 dilutions were used to generate the *Mmp2* primer standard curve. The 1:1 dilution returned an abnormally high Ct value, and the 1:8 dilution demonstrated a multiple-peaked dissociation curve. Both were consequently removed from the analysis. The standard curve slope for *Mmp2* was -1.0251 (see Figure 16). From this slope, the efficiency of *Mmp2* primers was calculated as 9.4518 using equation 1.

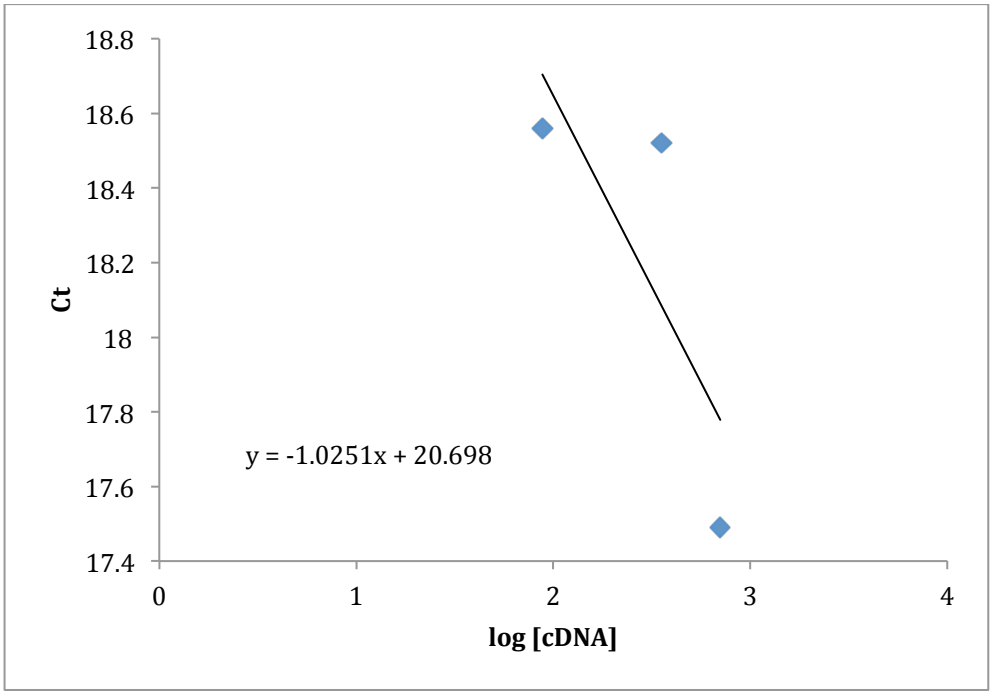

Figure 16. *Mmp2* primer standard curve. The log of serial diluted cDNA from whole body w^{1118} animals aged to 12 hours APF was plotted against DNA concentration in each serial dilution. The slope of the standard curve was used to determine the *Mmp2* primer amplification efficiency for the particular qPCR reaction. The slope of -1.0251 yielded an efficiency of 9.45.

Expression Ratios and Log Fold Change of qPCR Results Generated via the Pfaffl Method

A down-regulation of *Mmp2* expression was expected in *ßftz-f1*-reduced fat body at 8, 10, and 12 hours APF. Results from qPCR analysis were consistent with this expectation in 10 hour APF samples, but results from 8 and 12 hour APF samples were counter to the hypothesis. When examining qPCR expression ratios using the Pfaffl method, the wild-type expression ratio is always one. Expression ratios greater than one indicate over-expression, while expression ratios less than one indicate under-expression. The expression ratio at 8 hours APF was 4.24 indicating over-expression of *Mmp2* in *ßftz-f1*-reduced fat body as compared to w^{1118} fat body. The expression ratio at 10 hours APF was 0.0044 indicating a sizable under-expression of *Mmp2* in *ßftz-f1*-reduced bat body as compared to w^{1118} fat body. The expression ratio at 12 hours APF was 2.0643 indicating a slight over-expression of *Mmp2* in *ßftz-f1*-reduced fat body as compared to w^{1118} fat body (See Table 1).

In order to better visualize over vs. under expression of *Mmp2* in *ßftz-f1*-reduced fat body the results are presented as a figure comparing *Mmp2* expression ratios in *ßftz-f1*-reduced fat body to *Mmp2* expression ratios in wild-type fat body. (see Figure 17).

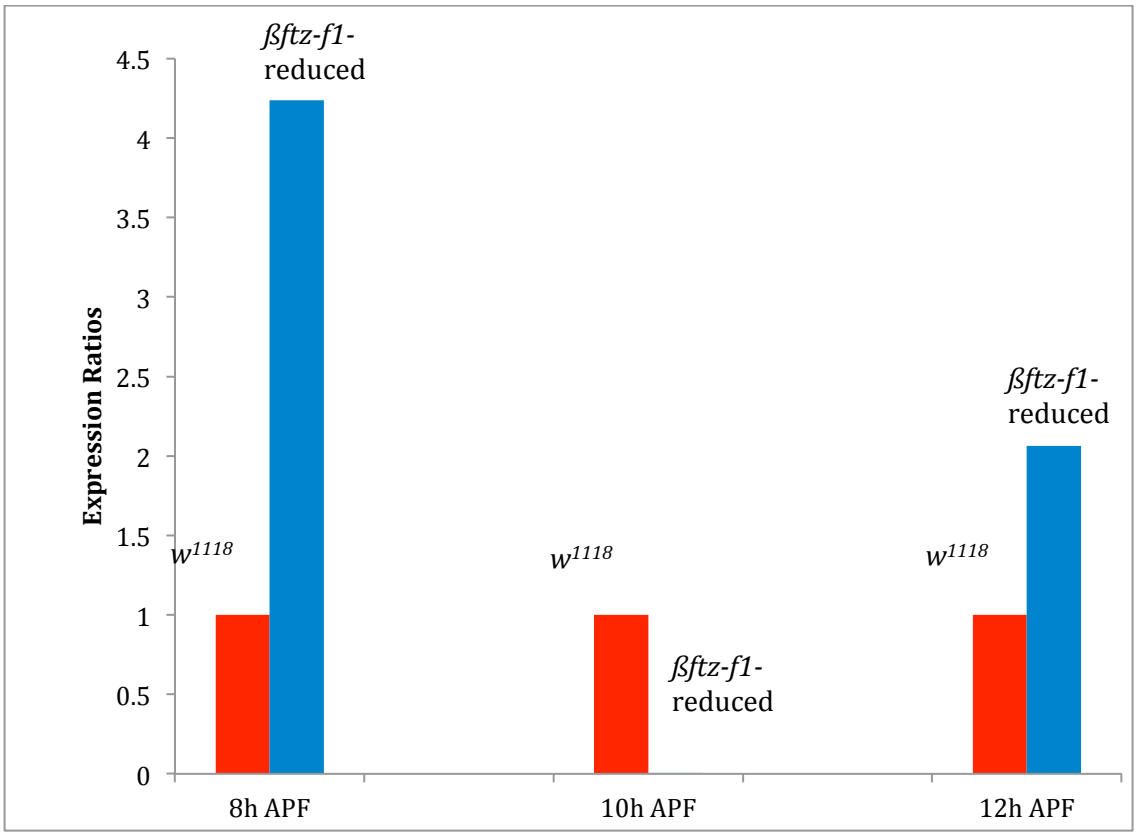

Figure 17. *Mmp2* expression ratios acquired from qPCR experiments. Expression ratios of *Mmp2* compared to *Actin 5c* expression in *ßftz-f1*-reduced compared to w^{1118} fat body are expressed in comparison to wild-type expression represented as a ratio of one. At 8 hours APF, the expression ratio is greater than one, indicating an over-expression of *Mmp2* in the larval fat body. At 10 hours APF, the expression ratio is less than one, indicating an under-expression of *Mmp2* in the larval fat body and support for the hypothesis. At 12 hours APF, the expression ratio is greater than one, indicating an over-expression of *Mmp2* in the larval fat body.

Results are also displayed as log fold change values. These values were acquired by taking the log of the expression ratios. These results represent over-expression as positive values (as observed in *ßftz-f1*-reduced fat body at 8 and 12 hours APF) and under-expression as negative values (as observed in *ßftz-f1*-reduced fat body at 10 hours APF). Looking at figure 18, the line at zero marks

wild type expression, while the bars extending above and below the line demonstrate the varied expression levels of *Mmp2* relative to *Actin 5c* in *ßftz-f1*-reduced fat body as compared to w^{1118} fat body at 8, 10, and 12 hours APF (see Figure 18). The figure clearly depicts the over-expression of Mmp2 in *ßftz-f1*-reduced fat body at 8 hours APF (log 4.2377 = 0.6271), the large under-expression at 10 hours APF (log 0.0044 = -2.3543), and the slight over-expression at 12 hours APF (log 2.0643 = 0.3148).

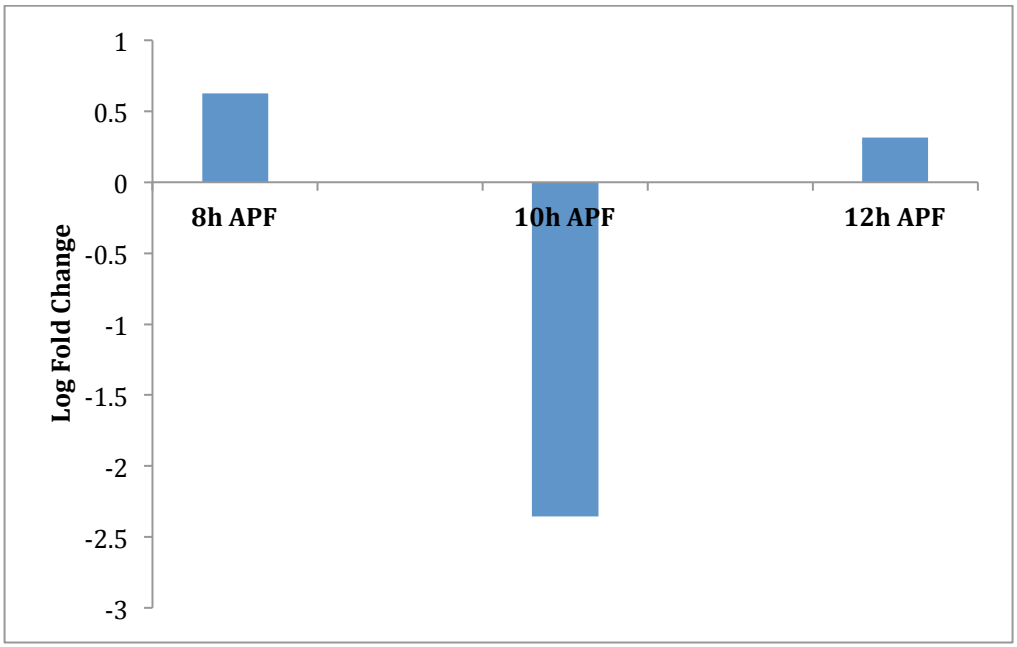

Figure 18. Log fold change of *Mmp2* expression relative to *Actin 5c* expression in *ßftz-f1*-reduced fat body as compared to w^{1118} fat body. Values were obtained by taking the log of the expression ratios generated using the Pfaffl method for qPCR analysis (see equation 2). Zero represents wild-type expression, therefore positive values indicate over-expression, and negative values indicate under-expression. The log fold change value of 0.6271 at 8 hours APF indicates over-expression of *Mmp2* in the larval fat body. The log fold change value of -2.3543 at 10 hours APF indicates under-expression of *Mmp2* in the larval fat body, and support for the hypothesis. The log fold change value of 0.3148 at 12 hours APF indicates over-expression of *Mmp2* in the larval fat body.

DISCUSSION

Dissection Observations

Observations were made during dissections of both w^{1118} and *ßftz-f1*-reduced fat body at all experimental time points. The general trend in the w^{1118} dissections was that fat body remodeling increased in positive correlation with later time points. These observations are consistent with the wild type progression of fat body remodeling. The general trend of the *ßftz-f1*-reduced fat body dissections was a reduction in fat body remodeling overall. Similar to observations in w^{1118} fat body dissections, fat body remodeling increased in positive correlation with later time points, however complete remodeling was never observed. Even in animals aged 12 hours APF, only partial remodeling was observed in *ßftz-f1*-reduced fat body dissections, whereas nearly full remodeling was observed in w^{1118} 12 hour APF fat body dissections. These observations are consistent with previously published findings (Bond et al., 2011).

These observations support my hypothesis. Animals with reduced *ßftz-f1* expression in the larval fat body demonstrated reduced larval fat body remodeling suggesting that a reduction/delay of *ßftz-f1* expression inhibits fat body remodeling, at least in part. These observations do not specifically demonstrate that this inhibition occurred via the proposed transcriptional cascade of ßFTZ-F1 conferring competence to *Mmp2* to respond to the prepupal ecdysone pulse to

translate MMP2 to degrade ECM allowing fat cell dissociation and detachment. These observations are, however, those expected in support of the hypothesis.

Reverse-Transcriptase PCR and Gel Electrophoresis

Results from RT-PCR and gel electrophoresis were overall successful. Some RT-PCR reactions yielded much stronger product than others. The varied strengths of visualized gel electrophoresis bands following RT-PCR amplification cannot be considered as quantifiable results. The only conclusions that can be drawn from gel visualizations are the presence of both *Mmp2* and *Actin 5c* mRNA transcript in all unique sample types, and the success of both cDNA synthesis and primer design. While not every gel showed both *Mmp2* and *Actin 5c* amplification bands, at least one gel (out of each set of three biological replicates) from every unique sample type demonstrated successful amplification of both genes. This demonstrates the presence, no matter the original expression level, of both *Mmp2* and *Actin 5c* mRNA in all sample types, as well as successful cDNA synthesis and primer design for those samples returning successful amplification images. Those samples that led to the most clearly defined visualizations of RT-PCR amplification were the samples chosen for use in qPCR.

Visualizations of both w^{1118} and *ßftz-f1*-reduced larval fat body cDNA synthesized from 8 hour APF samples demonstrated very clear bands from both *Mmp2* and *Actin 5c* RT-PCR amplification. These results clearly demonstrate the

presence of both *Mmp2* and *Actin 5c* mRNA in the *Drosophila* larval fat body at 8 hours APF in both wild type and *ßftz-f1*-reduced genotypes.

Previous RT-PCR experiments in the Woodard lab were not able to visualize successful RT-PCR amplification at 12 hours APF using the same genotypes as used in this study. Figures 14 and 15 demonstrate successful RT-PCR of samples collected from pupa aged 12 hours APF (see Figures 14 and 15). These images confirm the presence of both *Mmp2* and *Actin 5c* mRNA in the *Drosophila* larval fat body at 12 hours APF in both wild-type and *ßftz-f1*-reduced genotypes, as well as successful primer design and cDNA synthesis.

Mmp2 bands visualized in the w^{1118} 10 hour APF gels were much less clear than those of *Actin 5c*. This disparity in band brightness suggests a lack of success of *Mmp2* transcript amplification. That being said, the presence of even a weak band (as is depicted in Figure 11) confirms *Mmp2* mRNA presence, as well as successful cDNA synthesis and primer design. These results are supplemented by previous research in the Woodard lab demonstrating the presence of *Mmp2* mRNA in w^{1118} 10 hour APF fat body (see Figure 20). The presence of a weak *Mmp2* band, combined with successful amplification visualization from previous research confirms the presence of *Mmp2* mRNA in 10 hour APF *ßftz-f1*-reduced fat body. Images in this study demonstrated clear bands and successful RT-PCR amplification of 10 hour APF *ßftz-f1*-reduced *Actin 5c*, and *Mmp2* transcript, as well as of w^{1118} *Actin 5c* transcript (see Figures 12 and 13).

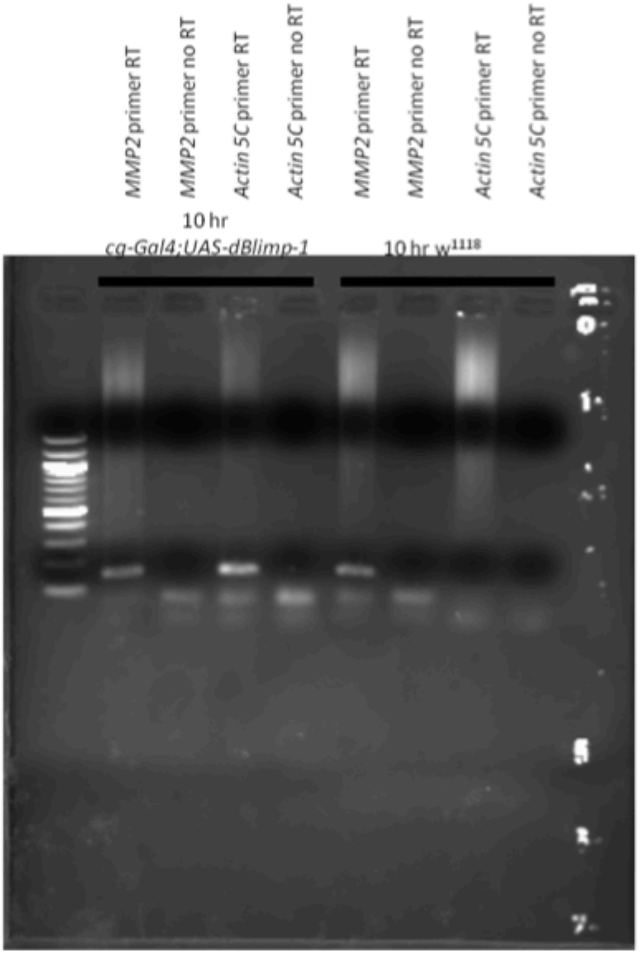

Figure 19. Gel image depicting PCR amplification of *Mmp2* and *Actin 5c* cDNA from-wild type and *ßftz-f1*-reduced fat body at 10 hours APF. This image was generated by previous research in the Woodard lab and demonstrates successful amplification of *Mmp2* cDNA from both wild type and *ßftz-f1*-reduced fat body. This research demonstrates the presence of *Mmp2* mRNA in 10 hour APF aged wild type and *ßftz-f1*-reduced fat body. Image from Pohl, (2014).

While one image of successful cDNA amplification was obtained for each time point, the study also yielded many unsuccessful images. For samples collected at 10 hours APF especially, acquiring a successful image was challenging; the final image was not especially clear. This phenomenon may have occurred for a number of reasons. Due to the faintness of the *Actin 5c* band

in some of the images that did not demonstrate successful *Mmp2* amplification, it is likely that challenges in obtaining successful images were not due to experimental alterations, but to inaccuracies in the experimental process. This challenge could be derived from a number of factors. It is possible that a mistake was made in the process of RNA isolation or cDNA synthesis. It is also possible that the *Mmp2* primer dilution used throughout the study expired, or was corrupted in some way over time, and was no longer functional when completing RT-PCR experiments later on in the experimental process.

What were interesting to observe were the similarities of images of both wild-type and *ßftz-f1*-reduced samples within experimental time points. This suggests that *Mmp2* expression variation is more strongly dependent on the stage of development (age of the pupa) than on the presence or absence of *ßftz-f1*. This suggestion however, is not likely. While developmental stage is an important factor in *Mmp2* expression regulation, evidence for *ßftz-f1* as a mediator of such regulation is quite widespread (Bond et al., 2011). Furthermore, *Mmp2* is not expressed in high concentrations in normal *Drosophila* development until 10-12 hours APF following the prepupal ecdysone pulse. This is evident in the knowledge that MMP2 carries out an essential physical action involved in fat body cell detachment, which is known to occur around 10-12 hours APF (Bond et al., 2011, Nelliot et al., 2006). The gel images from this study demonstrated the strongest *Mmp2* bands in samples collected from pupa aged to 8 hours APF in which *Mmp2* expression should be minimal. Eight hours APF is at the tail end of

the mid-prepupal period, before the rise in ecdysone stimulating *Mmp2* transcription (Bond et al., 2011, Woodard et al., 1994). Furthermore, RT-PCR and subsequent gel electrophoresis is not a quantitative method of measuring gene expression levels, and should not be considered a reliable source for observed quantitative analysis.

Potential Locations of Error

Sample collection and processing was carried out in three distinct rounds over the course of the study. Gel imaging results were successful for the majority of the samples included in the first and second rounds of sample processing, and unsuccessful for the majority of the samples included in the third round. This pattern suggests a mistake somewhere within the third round of processing. There were many steps involved in sample processing, and is possible that a mistake at one point in the process led to unsuccessful RT-PCR amplification.

RNA Concentrations

RNA concentration was measured for each sample both before and after DNase treatment. All samples maintained a concentration above 200, and a 260/280 value above 1.5 post-DNase treatments. While most samples were well above these marks, some samples were quite near the accepted minimums. Values closer to the minimum were observed more frequently in those samples obtained in the third round of sample collection and processing suggesting an

error in in RNA isolation or DNase treatment during this third round. Samples from 8 hour APF w^{1118} fat body dissections presented very successful visualizations of *Mmp2* and *Actin 5c* amplification corresponding with RNA concentration 260/280 values of above 1.8. Samples from 10 hour APF w^{1118} fat body dissections presented RNA concentration 260/280 values on the lower end of the spectrum, corresponding with a less prominent visualized *Mmp2* amplification. Results from 12 hour APF w^{1118} fat body samples support this reasoning. The gel visualizing 12h APF amplification of the sample collected in the first round of sample processing yielded an *Mmp2* band corresponding with an RNA concentration 260/280 value of above 1.7. The gel visualizing 12h APF amplification of the sample collected in the third round of sample processing, on the other hand, did not yield an *Mmp2* band, corresponding with an RNA concentration 260/280 value of below 1.7.

All *ßftz-f1*-reduced samples were processed in the second round. Some RNA concentration values from these samples were on the lower end of the acceptable spectrum, however nearly all gels visualized successful amplification of both *Mmp2* and *Actin 5c* template, and did not present any noticeable differences based on RNA concentration values.

cDNA Synthesis

One possible reason for challenges achieving RT-PCR amplification of *Mmp2* is unsuccessful cDNA synthesis. Many of the gels that did not

demonstrate successful PCR amplification of *Mmp2* transcript were run following the third round of sample processing. Most gels run following the first two rounds of sample processing demonstrated successful PCR amplification of both *Mmp2* and *Actin 5c* cDNA. It is possible that mistake was made in cDNA synthesis during the third round of processing. PCR primers were kept consistent throughout the study; the same stock dilution was used continuously, while cDNA varied, suggesting that the lack of successful amplification was not a result of un-successful primer design.

Primer Optimization

Another possible hindrance in achieving successful RT-PCR amplification of *Mmp2* transcript was the lack of focus placed on primer optimization in this study. Sample processing was carried out at three distinct times over the course of the study's progression, and the majority of results that yielded unsuccessful PCR amplification of *Mmp2* transcript occurred following the third of set these processing events. Throughout the study the same working dilution of *Mmp2* primers was used. It is possible that, over time, this working dilution of PCR primers was contaminated or corrupted in some way. Every time the dilution was used to set up RT-PCR reactions, it was put at risk of possible contamination – it is not unreasonable to consider that a once successful primer dilution expired or became corrupted over time.

In order to test this possibility, a working stock dilution of *Mmp2* that had achieved successful *Mmp2* transcript amplification in the past, was acquired from storage from previous use in the Woodard lab and used to run RT-PCR on cDNA that had failed to demonstrate successful Mmp2 transcript amplification (Pohl, 2014). These primers yielded similarly unsuccessful results, displaying images lacking a clear *Mmp2* band. This suggests that the problem lay in cDNA synthesis during the third round of sample processing, rather than in expired or corrupted primers. It is also possible that both the older working dilution, as well as the dilution used throughout the study were both corrupted in some way. More investigation is necessary in order to confirm either of these conclusions.

The stock dilution developed and used for the majority of this study was used to run qPCR experiments. Without full confirmation of the primers' continued legitimacy in the later parts of the experimental process, it is possible that, if the primer dilution did expire, it contributed to inaccurate qPCR results. qPCR results did demonstrate amplification of *Mmp2* transcript however, suggesting that the study's working *Mmp2* primer dilution had not expired. Without reliable confirmation of primer success, however, qPCR results cannot be considered fully reliable. Further investigation, primer optimization, and qPCR experimental replications are necessary for reliable results.

Quantitative Real-Time PCR Results

qPCR results demonstrate the expected down-regulation of *Mmp2* in *ßftz-f1*-reduced fat body in those samples collected from pupa aged 10 hours APF before dissection. qPCR results demonstrate an unexpected up-regulation of *Mmp2* in *ßftz-f1*-reduced fat body in those samples collected from pupa aged 8, and 12 hours APF before dissection. The observed down-regulation in 10 hour APF samples was very large, while both observed up-regulations, from 8 and 12 hour APF samples, were quite small (Both up-regulations were displaced with much less variation from wild-type expression ratios than was the large down-regulation observed in 10 hour APF samples. The up-regulation observed in 12 hour APF samples was even less than that observed in 8 hour APF samples.).

While these results do not fully support my hypothesis, at each time point there was a clear difference between *Mmp2* expression levels in wild-type fat body a compared to in *ßftz-f1*-reduced fat body – even if these differences did not unanimously demonstrate a reduction in *Mmp2* expression in *ßftz-f1*-reduced fat body. These results suggest a regulatory connection between *ßftz-f1* and *Mmp2*. *Mmp2* expression levels were altered, in comparison to wild-type expression, in experimentally developed transgenic flies over-expressing *dBlimp-1* in the larval fat body, without any direct experimental alterations to *Mmp2*. Previous research in the Woodard lab demonstrated a statistically significant reduction in *ßftz-f1* expression *in cg-Gal4; w; UAS dBlimp-1(XA)* flies, the same strain of experimentally developed transgenic flies used in this study to reduce *ßftz-f1*

expression (Perez, 2014). Since *dBlimp-1* has been significantly demonstrated as a *ßftz-f1*- repressor, it is fair to assume that experimental alterations led to changes in *ßftz-f1* levels and that those changes in *ßftz-f1* levels constituted the experimental alterations leading to the observed variations in fat body remodeling and *Mmp2* expression levels.

Considering this knowledge, this study demonstrates that altering *ßftz-f1* expression levels alters *Mmp2* expression levels in *Drosophila melanogaster* larval fat body. Wild-type and *ßftz-f1*-reduced samples underwent identical experimental procedures, therefore transgenic alterations, reducing *ßftz-f1* expression via over-expression of *dBlimp-1* affected *Mmp2* expression in the larval fat body. This demonstrates the connection between Mmp2 and *ßftz-f1*. Experimental parameters need to be optimized for reliable results demonstrating how this connection is manifested, as well as if down-regulation of *ßftz-f1* results in the expected down-regulation of *Mmp2.*

Possible Explanations for Unexpected qPCR Results

qPCR reactions were only carried out one time over the course of this study, eliminating any possibility of acquiring statistically significant data. As it was the first time qPCR had been run, some inaccuracies were easily noted from the beginning, such as slightly different reaction volumes observed in the plate (This was most likely a result of the previously mentioned miscalculation of the nuclease-free water volume in the *Actin 5c* master mix, and therefore likely had

no influence on final data). There was also one well that demonstrated a milky color rather than the clear of the rest of the reactions.

All samples demonstrated a melting temperature of above 80 °C suggesting a lack of primer dimer interruption. In contrast, much of the data demonstrated dissociation curves with multiple peaks suggesting primer dimer interruption. SYBR Green binds to any double stranded DNA within qPCR reactions, regardless of the length of the DNA strand. If primer dimer is present, SYBR Green will bind, fluoresce, and register as amplified transcript in data collection. qPCR measurements are taken in terms of fluorescence levels based on how much SYBR Green has bound to double stranded DNA regardless of whether or not it is bound to primer dimer or amplified transcript. If primer dimer is fluoresced in qPCR experiments and included in measurements of Ct values, Ct values will appear lower than accurate as the increased level of fluorescence will register as reaching the target transcript's threshold in fewer amplification cycles. This has the potential to interfere with qPCR results. Visualizations of RT-PCR results did include primer dimer in many samples, suggesting that dimer most likely had an effect on qPCR results.

Those samples that returned highly irregular dissociation curves were eliminated from the data. However, if all samples returning data with multiple-peaked dissociation curves were eliminated from the study, nearly 1/3 of all data would have been eliminated. Those samples returning double-peaked, closely associated, dissociation curves, but were otherwise normal, were included in data

analysis. It is important to note that many of the dissociation curves suggesting the potential presence of primer dimer were included in samples that yielded expected results. Many of these double-peaked dissociation curves were observed in qPCR amplifications of *Mmp2* transcript in cDNA from 10 hour APF w^{1118} fat body. This was the sample time that returned the expected reduction of *Mmp2* expression in *ßftz-f1*-reduced fat body.

Conclusions

In conclusion, results from qPCR experiments support the hypothesis in fat body samples aged 10 hours APF. Results from qPCR experiments are counter to the hypothesis however, in fat body samples aged 8 and 12 hours APF. These findings are highly preliminary. The presence of primer dimer and weak gel images at later points in the study suggest a possible corruption of the primers used in qPCR experiments. Due to the lack of replication of qPCR experiments, as well as the lack of primer optimization and subsequent double-peaked qPCR dissociation curves, the results are not reliable.

Results do not confirm nor deny the possibility of *Mmp2* as a downstream regulatory target of *ßftz-f1* in *Drosophila melanogaster* larval fat body remodeling. Results do demonstrate a connection of some kind between *ßftz-f1* and *Mmp2*, suggesting that *Mmp2* may indeed be a downstream regulatory target of *ßftz-f1*. Based on past research findings on this subject in support of the hypothesis, it is likely that the inconclusive results do not accurately demonstrate

the biological reality due to experimental inconsistencies and lack of replication. Further investigation is strongly encouraged in order to generate reliable and significant data demonstrating *Mmp2* as a downstream regulatory target of *ßftz-f1* in *Drosophila melanogaster* larval fat body remodeling.

Future Directions

Future actions should involve re-running RT-PCR using cDNA that returned successful amplification images from RT-PCR reactions run with the current working primer dilution. This would test for primer success – if cDNA that yielded successful amplification in the past fails to do so in the future, that is an indication that the working primer dilution has been corrupted. If cDNA that yielded successful amplification in the past continues to provide successful results, that is an indication that the cDNA synthesized in the third round of sample processing is invalid.

Future actions should also involve developing a new working dilution of *Mmp2* primers and re-running RT-PCR on cDNA that achieved successful amplification. If RT-PCR using the new primer dilution yields successful results, then that dilution should be used to re-run RT-PCR on those cDNA samples that did not yield successful amplification images in order to determine if the cDNA had been corrupted in any way. Once determining primer success, optimal primer and cDNA concentrations should be redefined with the aim of achieving an image without primer dimer. Ideal primer and cDNA concentrations that do not yield

primer dimer through RT-PCR will greatly increase the success and reliability of future qPCR experiments. Once identifying ideal primer and cDNA concentrations, many replications of qPCR experiments should be carried out in order to generate significant, reproducible data that accurately demonstrates the regulatory connection between *ßftz-f1* and *Mmp2* in *Drosophila* melanogaster larval fat body remodeling.

APPENDIX

Appendix 1. qPCR plate set up.

	1	2	3	4	5	6	7	8	9	10	11	12
A	Standard 1:1 *Actin 5c*	Standard 1:2 *Actin 5c*	Standard 1:4 *Actin 5c*	Standard 1:8 *Actin 5c*	Standard 1:16 *Actin 5c*	Blank	Blank	Blank	Blank	Blank	Blank	Blank
B	Standard 1:1 *Mmp2*	Standard 1:2 *Mmp2*	Standard 1:4 *Mmp2*	Standard 1:8 *Mmp2*	Standard 1:16 *Mmp2*	Blank	Blank	Blank	Blank	Blank	Blank	Blank
C	w^{1118} 8h *Actin 5c* RT	w^{1118} 8h *Actin 5c* RT	w^{1118} 8h *Actin 5c* RT	w^{1118} 8h *Actin 5c* no RT	Blank	Blank	Blank	Blank	*βftz-f1*-reduced 8h *Actin 5c* RT	*βftz-f1*-reduced 8h *Actin 5c* RT	*βftz-f1*-reduced 8h *Actin 5c* RT	*βftz-f1*-reduced 8h *Actin 5c* no RT
D	w^{1118} 8h *Mmp2* RT	w^{1118} 8h *Mmp2* RT	w^{1118} 8h *Mmp2* RT	w^{1118} 8h *Mmp2* no RT	Blank	Blank	Blank	Blank	*βftz-f1*-reduced 8h *Mmp2* RT	*βftz-f1*-reduced 8h *Mmp2* RT	*βftz-f1*-reduced 8h *Mmp2* RT	*βftz-f1*-reduced 8h *Mmp2* no RT
E	w^{1118} 10h *Actin 5c* RT	w^{1118} 10h *Actin 5c* RT	w^{1118} 10h *Actin 5c* RT	w^{1118} 10h *Actin 5c* no RT	Blank	Blank	Blank	Blank	*βftz-f1*-reduced 10h *Actin 5c* RT	*βftz-f1*-reduced 10h *Actin 5c* RT	*βftz-f1*-reduced 10h *Actin 5c* RT	*βftz-f1*-reduced 10h *Actin 5c* no RT
F	w^{1118} 10h *Mmp2* RT	w^{1118} 10h *Mmp2* RT	w^{1118} 10h *Mmp2* RT	w^{1118} 10h *Mmp2* no RT	Blank	Blank	Blank	Blank	*βftz-f1*-reduced 10h *Mmp2* RT	*βftz-f1*-reduced 10h *Mmp2* RT	*βftz-f1*-reduced 10h *Mmp2* RT	*βftz-f1*-reduced 10h *Mmp2* no RT
G	w^{1118} 12h *Actin 5c* RT	w^{1118} 12h *Actin 5c* RT	w^{1118} 12h *Actin 5c* RT	w^{1118} 12h *Actin 5c* no RT	Blank	Blank	Blank	Blank	*βftz-f1*-reduced 12h *Actin 5c* RT	*βftz-f1*-reduced 12h *Actin 5c* RT	*βftz-f1*-reduced 12h *Actin 5c* RT	*βftz-f1*-reduced 12h *Actin 5c* no RT
H	w^{1118} 12h *Mmp2* RT	w^{1118} 12h *Mmp2* RT	w^{1118} 12h *Mmp2* RT	w^{1118} 12h *Mmp2* no RT	Blank	Blank	Blank	Blank	*βftz-f1*-reduced 12h *Mmp2* RT	*βftz-f1*-reduced 12h *Mmp2* RT	*βftz-f1*-reduced 12h *Mmp2* RT	*βftz-f1*-reduced 12h *Mmp2* no RT

REFERENCES

Agawa, Y., Sarhan, M., Kageyama, Y., Akagi, K., Takai, M., Hashiyama, K., Wada, T., Handa, H., Iwamatsu, A., Hirose, S., and Ueda H. (2007). *Drosophila* Blimp-1 is a transient transcriptional repressor that controls timing of the ecdysone-induced developmental pathway. *Molecular and Cellular Biology, 27* (24), 8739-8747.

Aguila, J. R., Suszko, J., Gibbs, A. G., and Hoshizaki, D. K. (2007). The role of larval fat cells in adult *Drosophila melanogaster*. *The Journal of Experimental Biology, 210*, 956-963.

Akagi, K. and Ueda, H. (2011). Regulatory mechanisms of ecdysone-inducible *Blimp-1* encoding a transcriptional repressor that is important for the prepupal development in *Drosophila*. *Development, Growth & Differentiation*, *53,* 697–703.

Bainbridge, S. P., and Bownes, M. (1981). Staging the metamorphosis of *Drosophila melanogaster*. *Journal of embryology and experimental morphology, 66.1*, 57-80.

Bond, N. (2010). The role of ecdysone signaling in fat-body tissue remodeling and pupal metabolism. (Doctor of Philosophy, University of Nevada). (Public).

Bond, N. Nelliot, A., Bernardo, M.D., **Gorski, K., **Ayerh, M., Hoshizaki, D.K. and Woodard, C.T. (2011). ßFTZ-F1 and Matrix metalloproteinase 2 are required for fat-body remodeling in *Drosophila. Developmental Biology, 360,* 286-296.

Broadus, J., McCabe, J.R., Endrizzi, B., Thummel, C.S., and Woodard, C.T., (1999). The *Drosophila* βFTZ-F1 orphan nuclear receptor provides competence for stage-specific responses to the steroid hormone ecdysone. *Mol. Cell, 3,* 143-149.

Campbell, N. A., Reece, J. B., and Meyers, N. *Biology*. Frenchs Forest, N.S.W.: Pearson Education, 2005. Print.

Caterina, J. J., Yaada, S., Caterina, N. C. M., Longenecker, G., Holmback, K., Shi, J., Yermovsky, A. E., Engler, J. A., and Birkednal-Hansen, H. (2000). Inactivating mutation of the mouse tissue inhibitor of Metalloproteinases-2 (Timp-2) gene alters ProMMP-2 activation. *Biol. Chem.*

Coussens, L. M., Fingleton, B., and Matrisian, L. M. (2002). Matrix metalloproteinase inhibitors and cancer: trials and tribulations. *Science, 295* (5564), 3287-2392.

Duffy, J. B. (2002). *GAL4* system in D*rosophila*: A fly geneticist's swiss army knife. *Genesis, 34*, 1-15.

Fortier, T.M., Vasa, P.P., and Woodard, C.T. (2003). Orphan nuclear receptor βFTZ- F1 is required for muscle-driven morphogenetic events at the prepupal–pupal transition in *Drosophila melanogaster*. *Dev Biol. 257*, 153-165.

Géminard, C., Rulifson, E. J., and Léopold, P. (2009). Remote control of insulin secretion by fat cells in *Drosophila*. *Cell metabolism 10.3*, 199-207.

Gialeli, C., Theocharis, A.D., and Karamanos, N.K. (2011). Roles of Matrix metalloproteinases in cancer progression and their pharmacological targeting. *FEBS Journal, 278*, 16-27.

Hyun-Jeong, R., and Parks W. C. (2007). Control of Matrix metalloproteinase catalytic activity. *Matrix Biology 26.8,* 587-96.

Kessenbrock, K., Plaks, V., and Werb, Z. (2010) Matrix metalloproteinases: regulators of the tumor microenvironment. *Cell, 141.1*, 52-67.

Kozlova, T, and Thummel, C. S. (2003). Essential roles for ecdysone signaling during *Drosophila* mid-embryonic development. *Science, 301.5641* 1911-914.

Lu, P., Takai, K., Weaver, V. M., and Werb, Z. (2011). Extracellular matrix degradation and remodeling in development and disease. *Cold Spring Harbor Perspectives in Biology 3.12*.

Lu, P., Weaver, V. M., and Werb, Z. (2012). The extracellular matrix: a dynamic niche in cancer progression." *The Journal of Cell Biology 196.4*, 395-406.

Nelliot, A., Bond, N., and Hoshizaki, D. K. (2006). Fat-body remodeling in D*rosophila melanogaster*. *Genesis, 44*(6), 396-400.

Page-McCaw, A. (2008). Remodeling the model organism: Matrix metalloproteinase functions in invertebrates. *Seminars in Cell & Developmental Biology, 19*, 14-23.

Page-McCaw, A., Ewald, A. J., and Werb, Z. (2007). Matrix metalloproteinases and the regulation of tissue remodeling. *National Review of Molecular Cell Biology, 8*, 221- 233.

Page-Mccaw, A., Serano, J., Sante, J., and Rubin, G. (2003). *Drosophila* Matrix metalloproteinases are required for tissue remodeling, but not embryonic development. *Developmental Cell, 4.1*, 95-106.

Perez, L. (2014). *The effects of ßftz-f1 in Drosophila melanogaster larval fat body remodeling.* Unpublished Bachelors of Arts, Mount Holyoke College.

Pfaffl, M.W. (2001). A new mathematical model for relative quantification in real-time RT-PCR. *Nucleic Acids Res*, *29* (9).

Papelexi, E. (2013). The genetic control of fat body development and function in *Drosophila melanogaster.* Unpublished Bachelors of Arts, Mount Holyoke College.

Pohl, N. (2014). *The Role of MMP2 in Drosophila melanogaster fat body remodeling.* Unpublished Bachelors of Arts, Mount Holyoke College.

Qiangqiang, J., Yang, L., Hanhan, L., and Sheng, L. (2014). Mmp1 and Mmp2 cooperatively induce *Drosophila* fat body cell dissociation with distinct roles. *Scientific Reports, 4* (7535).

Rao, X., Lai, D., and Huang, X., (2013). A new method for quantitative real-time polymerase chain reaction data analysis. *Journal of Computational Biology, 20,* 703-711.

Stephenson, R., and Metcalfe, N. H. (2013). *Drosophila melanogaster*: A fly through its history and current use. *Journal of the Royal College Physicians Edinburgh, 43*, 70-75.

Stevens, L. J., and Page-Mccaw, A. (2012). A secreted MMP is required for re-epithelialization during wound healing. *Molecular Biology of the Cell 23.6*, 1068-079.

St Johnston, D. (2002). The art and design of genetic screens: *Drosophila melanogaster*. *Nature Reviews Genetics 3,* 176-188.

Timofeev N. P. (2008). Ecdysteroids: usage in medicine, sources, and biological activity (review). *Voprosy Meditsinskoi Khimii (Biomedical Chemistry) 50*, 133-152.

Weigmann, K., Klapper, R., Strasser, T., Rickert, C., Technau, G. M., Jackle, H., Janning, W., and Klämbt, C. (2003). FlyMove: A new way to look at development of *Drosophila*. *Trends Genetics, 19* (6), 310-311.

White, K. P., Hurban, P., Watanabe, T., and Hogness, D. S. (1997). Coordination of *Drosophila* metamorphosis by two ecdysone-induced nuclear receptors. *Science, 276*, 114-117.

Woessner, J. F. Jr. (1991) Matrix metalloproteinases and their inhibitors in connective tissue remodeling." *The FASEB Journal 5.8*, 2145-2154.

Woodard, C. T., Baehrecke, E. H., and Thummel, C. S. (1994). A molecular mechanism for the stage specificity of the *Drosophila* prepupal genetic response to ecdysone. *Cell, 79*, 607-615.

Yamada, M., Murata, T., Hirose, S., Lavorgna, G., Suzuki, E., and Ueda, H., (2000). Temporally restricted expression of transcription factor betaFTZ-F1: significance for embryogenesis, molting and metamorphosis in *Drosophila* melanogaster. *Development 127*, 5083-5092.

Yuan, J. S., Reed, A., Chen, F., Stewart, C. N. Jr. (2006). Statistical analysis of real-time PCR data. *BMC Bioinformatics 7* (85).